THE UNIVERSITY OF MANITOBA

A RAPID TECHNIQUE FOR DETERMINING BINARY AND TERNARY PHASE DIAGRAMS

by

Bo Lind Mikkelsen

A THESIS

SUBMITTED TO THE FACULTY OF GRADUATE STUDIES

IN PARTIAL FULFILMENT OF THE REQUIREMENTS FOR THE DEGREE

OF MASTER OF SCIENCE IN ENGINEERING (MECHANICAL)

DEPARTMENT OF MECHANICAL ENGINEERING

WINNIPEG, MANITOBA

OCTOBER, 1971.

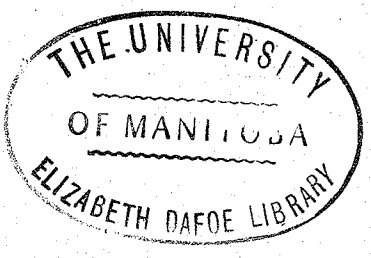

INDEX PAGE

INDEX PAGE

ABSTRACT

A method has been developed for phase diagram determination by means of electron microprobe analysis of liquid diffusion couples. The method was tested on the Al-Mg binary system, and then used to determine the isothermal section at 535°C of the Al (rich) corner of the Al-Cu-Ni system up to Al-50wt% Ni and Al-52 wt%Cu. This investigation was initiated after research on an Al(rich)-Cu-Ni structural alloy showed that existing phase diagrams for the Al-Cu-Ni system were in error. The technique described can be used to establish isothermal sections of a binary or ternary alloy system in a few weeks. Considerable information concerning the liquid-solid reactions can also be gained using this technique.

LIST OF FIGURES

LIST OF TABLES

1. INTRODUCTION

Constitutional, or phase diagrams, are used extensively in every aspect of metallurgy. They are used to produce materials of defined and controlled physical properties, in solidification, in purification such as zone refining, to determine thermodynamic data, and a host of other uses.

With new materials and alloys being developed, their phase diagrams are in turn required to control their usage. The science of phase diagramming is thus in constant demand. This science has benefitted from the technological advances in the area of material analysis, but has not otherwise progressed significantly since the book by Hume-Rothery et al (12). Researchers, in determining a phase diagram, are casting up literally hundreds of samples of varying composition to produce tiny parts of a phase diagram. One researcher, who did some of the founding work on the Al-Cu-Ni diagram, used seventy-eight samples of differing composition (2) to produce a phase diagram of the Al-Cu-Ni system up to Al-12 Cu and Al-10Ni which is less than 1.5% of the whole system. To quote Hume-Rothery et al (12).

> "The determination of a complete ternary diagram so as to establish the liquidus, solidus, and solid solubility relations over a wide range of temperature involves much work. In all but the most simple systems the complete determination will occupy two whole-time workers for at least four years, and with difficult systems as much as five to ten years work may be involved."

Clearly a quicker method, which can render both a qualitative determination as well as a detailed analysis of the phase diagram, is required. Delays in the order of years are undesirable in materials development. Furthermore, it is reasonable to speculate that alloy development has been retarded due to the lack of phase diagrams and the reluctance of researchers to embark on such tedious research projects.

A method of phase diagram determination has been developed in this investigation involving liquid diffusion couples, by which any number of isothermal sections can be determined from the sample. In simplest terms the method consists of producing a diffusion couple with the concentration of elements varying across the portion of the diagram being investigated, heat treating, then performing microscopic and electron microprobe analysis of the couple.

Since solid state diffusion is relatively slow, and not all phases appear due to differences in diffusion rates (eg. in the Al-Zr system only Al_3Zr forms (14)), the couples are made by liquid diffusion. The exact method of making the couples varies with the physical and chemical properties of the elements involved. As many couples as are deemed necessary can be made, but for binary systems one will often suffice, using the pure elements as the ends of the couple. For ternary systems couples can be taken across the corners of the diagram. Through liquid diffusion, the concentration of each element will vary from maximum to zero along the length of the couple. This concentration gradient gives rise to all phases in the system and upon heat treatment they assume their equilibrium configuration. Then by the use of electron probe microanalysis the exact phase compositions, and phase field boundaries can be established. Even if equilibrium has not been established, tie lines can be established by measuring interface compositions of the

coexisting phases (7). By heat treatment at various temperatures each isothermal section can be produced. While the method is most powerful for determining isothermal sections in the solid, considerable information concerning the liquidus may also by obtained.

The method resulted from research concerning unidirectionally solidified Al-Cu-Ni ternary alloys. A strong phase was desired which could solidify in a fibre aspect, producing a fibre reinforced material. Al(rich)-Ni fibre reinforced alloys have been produced which have attractive properties (15). In these alloys the reinforcing phase is $\varepsilon(Al_3Ni)$ which has a strength in the order of 400,000 psi (15). The δ phase, a higher nickel phase (Al_3Ni_2), has a higher melting point than ε(1100^{o} vs $1400^{o}C$) and therefore may be a stronger phase. While it is impossible to produce Al-δ composites in the binary system, existing ternary diagrams (18) for the Al-Cu-Ni system indicate that an Al-δ region does exist in this system. Initial attempts to produce such alloys from these ternary diagrams were frustrated, and it was concluded that these diagrams were inaccurate. Hence a quantitative analysis of the Al-Cu-Ni system was required and since conventional methods would have proved much too time consuming, the present method was developed.

This method was tested on the binary Al-Mg system, and then used to establish the isothermal section of the Al-Cu-Ni diagram at $535^{o}C$ up to Al-50Ni and Al-52Cu. The total time for development of the process and analysis of the two isothermal sections was less than six months.

2. PRINCIPLES OF PHASE DIAGRAMMING

Phase diagrams are graphs of the state of material using the independent variables of composition, temperature and pressure. They are classified by the number of components, i.e. two elements are binary systems, three elements are ternary systems, etc. From consideration of thermodynamic principles, and also from actual phase diagrams, certain rules governing the construction of these diagrams have been formulated.

2.1 Binary Systems

Binary diagrams established at constant pressure require two dimensions for representation - one for temperature, and one for the dependently varying composition. The details of the diagram are governed by the following:

i) The Phase Rule - (originally due to Gibbs) in a system under equilibrium the sum of the number of phases (p) plus the number of degrees of freedom (f) equals the number of components (C) plus two.

ie) $p + f = C + 2$, or for constant pressure, $p + f = C + 1$

where:

phase - is any portion of a system (including the whole) that is physically homogeneous within itself and is bounded by a surface so that it is mechanically separable from any other portions (16).

components - are the smallest number of independently variable constituents required for the statement of the compositions of all phases of a system (26).

degrees of freedom - the number of conditions that can be varied independently without changing the state of the system, or which have to be stated to completely define the state of the system (26).

ii) Boundary Rule - any region containing p phases can only be bounded by regions containing p + 1 or p - 1 phases (where p is the number of phases) (9).

iii). The Boundary Curvature Rule - Boundaries of one-phase regions must meet with curvatures such that the boundaries extrapolate into the adjacent two-phase regions (9).

iv) The Solubility Rule - all components are soluble to some degree in all phases (9).

2.2 Ternary Systems

To represent phase equilibria in a ternary system (at constant pressure) requires a triangular prism - the three equilateral legs representing the binary systems of the component elements, and the vertical axis representing temperature. It is possible to form ternary phases, but often the ternary system consists only of phases that are found in the three binary systems. The following apply to, and govern a ternary phase diagram.

i) the phase rule - as explained in 2.1.

ii) Law of adjoining phases - which regards the number of phases in a region in relation to its neighbouring regions in a phase diagram of n components.

$$R_1 = R - D^- - D^+ \geq 0 \qquad (26)$$

where:

R_1 - is the dimension of the boundary between neighbouring phase regions eg. for a point $R_1 = 0$, for a line $R_1 = 1$.

R - is the dimension of the concerned diagram or section of a diagram eg. for an isothermal section of a ternary diagram R = 2.

D^+ - is the number of phases that appear in crossing the boundary

from one phase region to another.

$\bar{D}$ - is the number of phases that disappear in crossing the boundary from one phase region to another.

From this formula the following rules arise which apply to a two dimensional section of a ternary diagram.

a) A one-phase region joins a two-phase region along a line.

b) A one-phase region joins a three-phase region at a point.

c) A two-phase region joins with a three-phase region along a tie line.

d) A two-phase region joins a two-phase region at a point.

e) A one-phase region joins a one-phase region at a point.

iii) A three-phase field is a triangle, bounded on all sides by two phase regions. The composition of each phase in a three-phase region is given by the composition at the corners of the triangle.

iv) A two-phase region is four sided, and bounded by tie lines.

v) Tie lines are established experimentally and join regions of phases in equilibrium with each other. Tie lines at different isothermal sections may run in different directions, and hence would not lie in the same vertical section.

3. CONVENTIONAL PHASE CHARACTERIZATION

3.1 Phase Identification Techniques

3.1.1 Optical Microscopy (12)

This classical technique of examining materials is a very powerful one due to the many innovations that have been introduced. The different types of illumination such as dark field, oblique light, opaque

stop, phase contrast, polarized light microscopy, and interferrometry result in a variety of ways to examine a specimen - and a variety of characteristics to examine.

A specimen is prepared for light optics examination by polishing (mechanical, chemical, electro chemical) and etching (chemical, electro chemical). The specimen may then be examined under direct illumination, or by any of the techniques mentioned above. With judicious etching, features such as grain boundaries, different phases, eutectic and peritictic reactions, characteristic formations such as twinning, and slip bands may also be observed. All of these features, as well as differences in micro hardness tend to differentiate and identify phases. Such examination thus gives a qualitative analysis of the phase diagram in terms of phases present, phase boundaries, phase transformations and general composition gradients.

Optical microscopy, although yielding a general analysis, is not sufficient for quantitative analysis. Due to limited powers of resolution, small particles or precipitates may not be detected, or some different phases may react identically to etching techniques, and hence be mistaken for the same phase. Consequently other analytical techniques must be used to confirm microscopic determinations. Other problems, such as particles falling out of brittle matrices, or reactive alloys decomposing when in contact with polishing compounds arise during preparation of alloys for examination.

3.1.2 X-Ray Diffraction Technique (12) (17)

X-ray diffraction techniques, on powder specimens or polycrystalline aggregates, are used to determine the composition of phases, as well as yielding information on the crystal lattice. The material to be examined, especially by the Debeye Scherrer method, is generally ground to a powder, annealed, and subjected to "monochromatic" radiation of a predetermined wavelength. The material then gives off a diffraction pattern characteristic of the particular material. From this pattern can be determined not only the phase relations of the alloy, but also its lattice parameters, crystal system and type, and whether ordering exists.

This is a general technique used in the conventional phase characterization method to confirm analysis done by optical microscopy. The method also yields information on phase boundaries through a variation in lattice spacing with atomic composition.

3.1.3 Electron Microscopy (23)

Providing that a thin($\sim$100Å) foil of the material can be made, transmission electron microscopy may also be used to identify a material. An incident electron beam produces a diffraction pattern following the same crystallographic criteria as X-rays. Hence a material may be analyzed by deciphering this electron diffraction pattern. Since the diffraction pattern is produced from the area that the electron beam impinges upon, smaller ($\sim$ 10Å diameter) particles such as precipitates may be identified.

3.1.4 Electron Probe Microanalysis (3)

The electron microprobe, using a focussed beam of electrons to excite characteristic X-radiation from areas .1 to 3 μ diameter, is

one of the most powerful and diversified compositional analysis tools available.

"....in fact, virtually anything from telephone pole quality control to forensic medicine is or has been performed with the aid of the microprobe". (25)

With X-ray optics, the characteristic radiation from the sample is collected and analyzed according to wavelength and intensity. Depending on the standards used, this data is modified by correction factors (absorption, flourescence, atomic number) (6), and compared to the standard. Probes may be linked to a computer for analysis of intensity data (6). The practical limit of analysis is about 100 ppm. (3), or in terms of actual amounts about 10^{-15} grams based on .01 wt.% in a specimen of 10^{-11} gms (5). Since these concentrations are very localized, for example in the size of precipitates or inclusions, this may represent parts per billion when considered over the whole sample.

There are, however, other limits placed on the analysis. For elements below Na, atomic number eleven, the X-radiation is difficult to detect and is affected by chemical bonding and the physical state of the element. Through the use of special diffracting crystals, however, carbon (at. no. 6) can be analyzed. Another problem is in analyzing for elements for which there is lack of accurately determined parameters, such as mass absorption coefficient. The accuracy limit imposed on specimens containing these less common elements acts as a constraint to more intensive reliance on microprobe analysis in the study of phase diagrams (5). By the proper choice of standard, however, the problems of some correction factors, such as for mass absorption, vanish.

Notwithstanding these shortcomings, the probe is extremely beneficial for phase diagramming. In ternary diagrams, the extent of

a three-phase region can be determined from composition of the three coexisting phases, tie lines can be obtained directly by measuring the composition of two existing phases at equilibrium (7).

Furthermore, the probe can make use of such auxiliary techniques as cathode luminescense, sample and backscatter electron currents, secondary emission, and Kossel divergent beam microdiffraction for analysis.

3.1.5 Other Techniques

Several other techniques dealing with physical, crystallographic and molecular characteristics of the phases such as Mossbauer spectroscopy, neutron diffraction, nuclear mass resonance, D.C. magnetic susceptibility, Hall coefficient, elastic constant, and X-ray absorption edge spectroscopy are also used in phase identification.

3.2 Phase Boundary Determination

3.2.1 Thermal and Differential Thermal Analysis (12) (17)

Although phases have definite isothermal compositional boundaries a change in temperature brings changes in structures, solid solubilities, and the compositional boundaries of the phase. One method of locating these phase boundaries is by thermal analysis.

Thermal analysis utilizes the latent heat or changes in specific heat which accompany structure changes. By establishing the temperature versus time graph upon heating and/or cooling, any inflection point, or change in slope could denote a phase change. This is generally accomplished by thermocouples embedded in samples, and by motor driven rheostats to give constant heating rates. This technique is very good for determining liquidus lines.

Another technique, dependent upon the same principles is differential thermal analysis (DTA). In DTA a thermocouple is placed both in the specimen and in a standard which has no phase change in the region under observation. The two thermocouple emfs are then subtracted (differential) and the combination is amplified. This technique is very sensitive to phase change, and is better than thermal analysis for solidus determination.

3.2.2 Electrical Conductivity (12) (17)

For subsolidus phase analysis, electrical conductivity is more sensitive to phase change than DTA. Since it does not depend on spontaneous heat effects, this method can allow a finite time for equilibrium to be established. The technique depends on the change in conductivity with a structural or phase change. Hence changes in σ vs T curves will occur at phase changes. There are different experimental techniques for different materials, but the important factors are constant geometry of specimen and ohmic contact throughout the temperature range investigated.

3.3.3 Incipient Melting (11)

This technique is used for determining solidus temperatures. The test is accomplished by heating the specimen in a suitable furnace (11) until signs of melting appear. The temperature is noted and other specimens are heated to specific temperatures below the observed melting and quenched. These specimens are then prepared for optical microscopy, and signs of incipient melting observed. The highest temperature where signs of melting are absent is the solidus.

3.3.4 Other Techniques (17)

Other techniques which utilize the property changes in phases to determine the position of phase changes are thermal gravimetric analysis, vapour pressure measurements, EMF measurements on galvanic cells involving solid electrolytes, dilatometric techniques (12) and high pressure, high temperature X-ray diffraction. Computer calculations using thermodynamic considerations have also been used to establish ternary phase diagrams (13). The use of the theoretical treatment for phase diagramming, however, is restricted by the lack of appropriate thermodynamic data and an incomplete understanding of the thermodynamics of intermetallic compounds.

4. PREVIOUS RESEARCH ON PHASE DIAGRAMS

4.1 Al-Mg System

This system is well represented in Hansen (10) together with the analysis of each phase. The only doubt appears to be concerning ε phase in the $\beta + \gamma$ region (refer to Fig. 1). The stability and range of existence of ε are apparently not certain.

4.2 Al-Cu-Ni System

Some of the first work on the Al-Cu-Ni system was performed by Bingham and Haughton (2) who were motivated by research on a ternary structural alloy. Using thermal analysis, high temperature resistance measurements, and microscopical examination they determined the phase diagram up to Al-12%Cu and Al-10%Ni. Their findings were presented in terms of vertical sections across the phase diagram at both constant copper

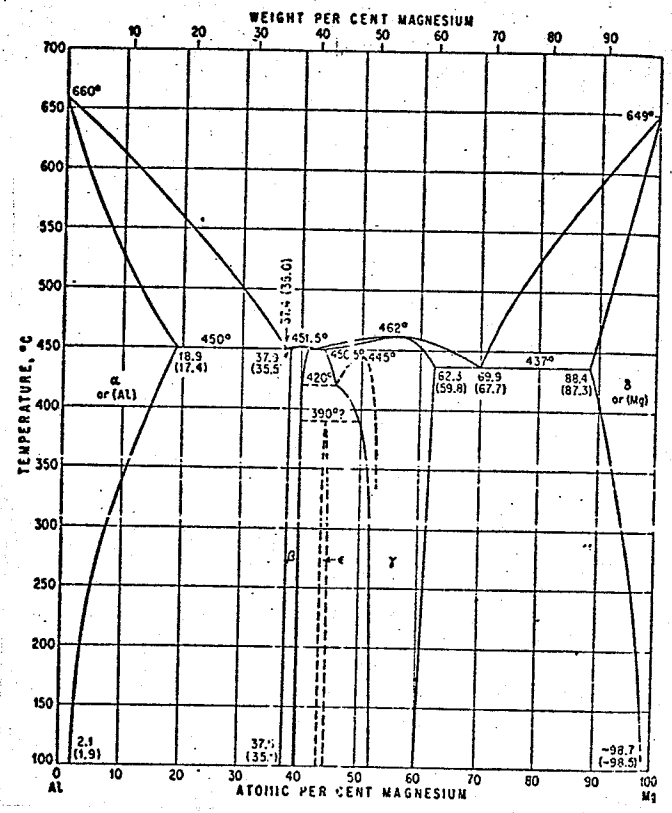

Figure 1. Al-Mg Binary Phase diagram-Hansen (10)

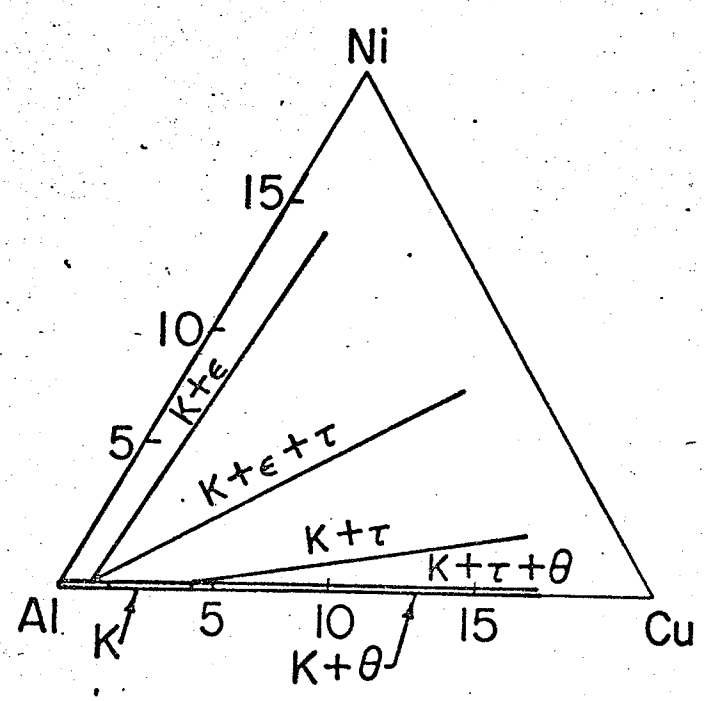

FIGURE BINGHAM & HAUGHTON'S ( ) ISOTHERMAL OF Al-Cu-Ni SYSTEM AT 535° C

and constant nickel concentrations. They reported four phases:

*κ - aluminum solid solution

θ - $CuAl_2$, a stoichiometric compound of aluminum and copper

ε - $NiAl_3$, a stoichiometric compound of aluminum and nickel with limited solubility of copper

τ - a ternary constituent centering upon Cu_2NiAl_5

From the vertical sections presented, the isothermal section in fig. 2 for 535°C may be constructed. At about this same time Austin and Murphy (6) using thermal analysis established the liquidus (fig. 3) and parts of the solidus for the entire Al-Cu-Ni system.

Bradley and Lipson (4) undertook an investigation of slowly cooled alloys of the whole Al-Cu-Ni system by X-ray techniques. They also reported the existence of the ternary constituent τ in the Al (rich) corner of the system (fig.4

They proposed Cu_3NiAl_6 as the simplest formula for τ and gave its crystal structure from X-ray investigation as deformed body centered cubic. They also found δ - Ni_2Al_3 to $NiCuAl_3$ (trigonal) in the Al-rich corner of the system, to bring the total number of phases to five, i.e. $\kappa,\varepsilon,\delta,\theta$ and τ. This diagram that Bradley and Lipson determined is the one recorded in the Metals Handbook (18).

Rapp (21) worked in the Al-rich corner of the Al-Cu-Ni system. He presented an isothermal section at 530°C of the system to Al 30 Cu and Al-25Ni (fig. 5).

Aside from the previously determined phases of $\kappa,\theta,\varepsilon$ and τ, he proposes two others Y and Z. Both of these new phases being ternary constituents, and both being formed peritectically. He has also determined the solid and liquid reactions in the Al (rich) corner and shows them, as well as their temperatures, in a liquidus projection on the base triangle (fig. 6). Both microscopical

* The symbols for the phases is similar to that in the Metals Handbook (18).

and X-ray techniques were used in his determination, and he has shown micrographs of both as cast and heat treated structures.

After considering the diverse diagrams that have been researched it is reasonable to conclude that some confusion exists concerning the nature of the Al (rich) corner of the Al-Cu-Ni system.

5. PRINCIPLES OF LIQUID DIFFUSION COUPLE TECHNIQUE

5.1 Binary Systems

Consider the principle of liquid-diffusion couple phase diagram analysis by visualizing in turn a binary and a ternary system.

The binary system AB (fig. 7) is bounded by the elements A and B. Consider a liquid diffusion couple made from A and B. Upon melting there may be initial convective mixing at the interface between the two metals but after melting was complete, liquid diffusion would take over as the dominant material transport mechanism. This would produce a concentration gradient much like a Boltzman Matano curve (fig. 8a). Consider solidification of individual compositions in the couple, e.g. x_1 in Figure 7. Assuming that the solidification rate is fairly rapid, composition x_1 will yield cored α plus eutectic, E_1. In fact every composition from pure A to E_1 will give cored α plus E_1. Furthermore, compositions E_1 to x_2 will give cored β plus E_1, compositions x_2 to E_2 will give cored β plus E_2, compositions E_2 to pure β will give cored γ plus E_2. Hence the couple, in the as solidified state, should give the alternating fields indicated in fig. 8a'. From this couple the solidus reactions, such as eutectics and number of phases present may be observed.

Upon heat treatment at some temperature, T, below T_2 a uniform

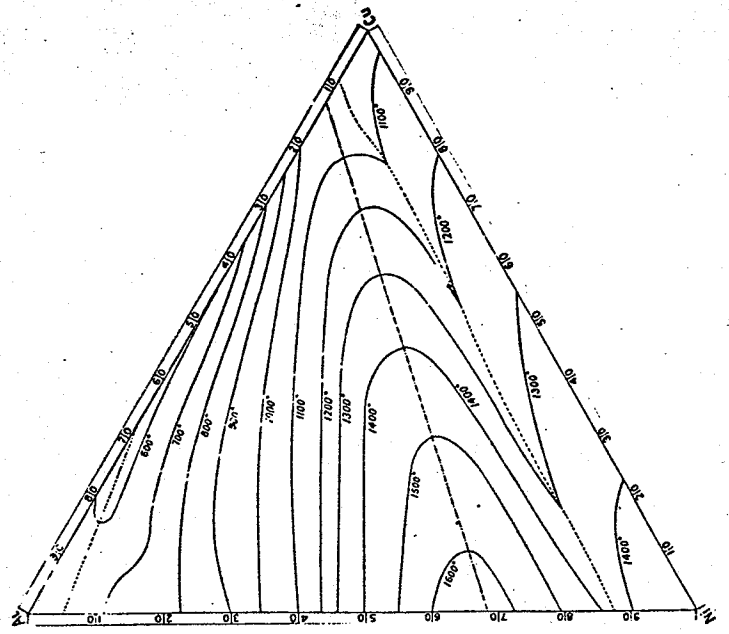

Figure 3. Liquidus of Al-Cu-Ni System (1)

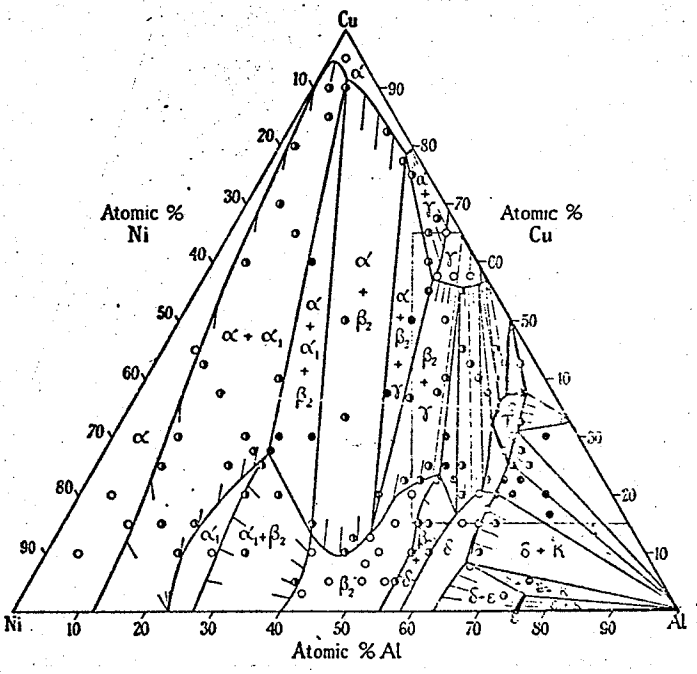

Figure 4. Al-Cu-Ni System from Bradley & Lipson (4)

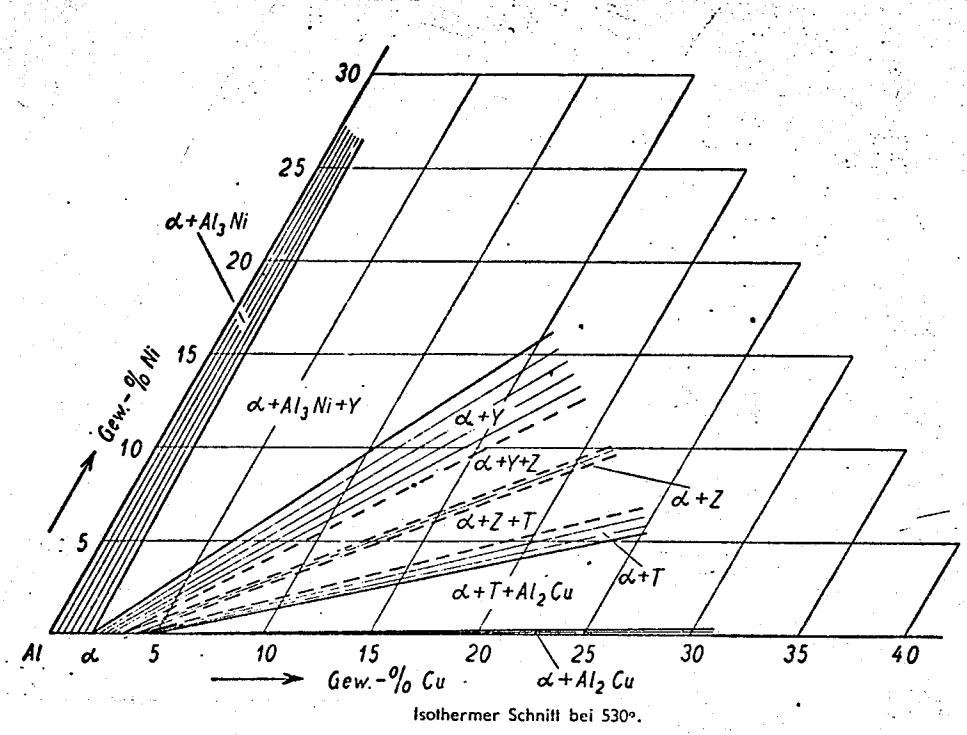

Figure 5. Isothermal Section of Al-Cu-Ni system at 530°C from Rapp (21).

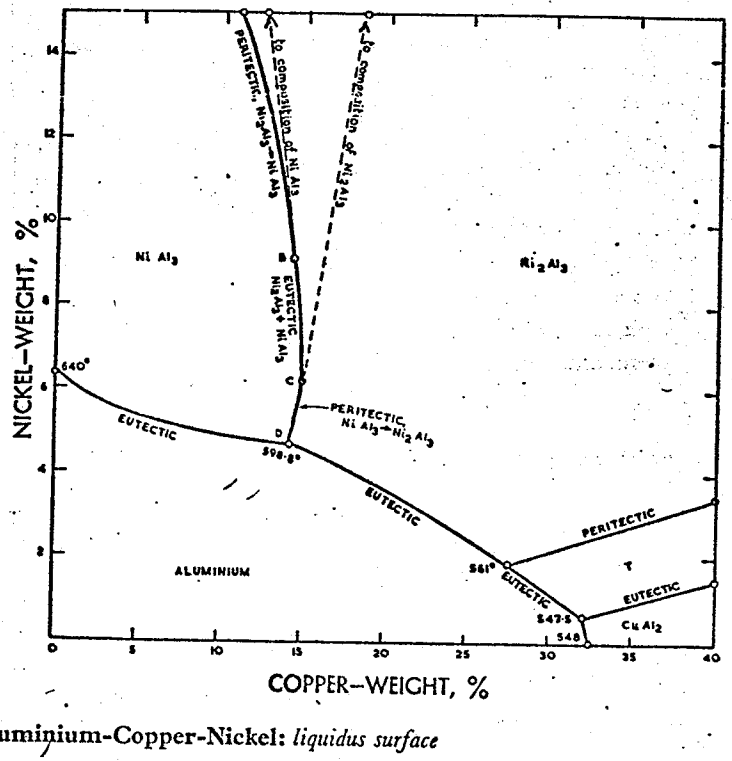

Aluminium-Copper-Nickel: *liquidus surface*

Figure 6. Projection of Liquidus Surface on the Base of Al-Cu-Ni diagram (8)

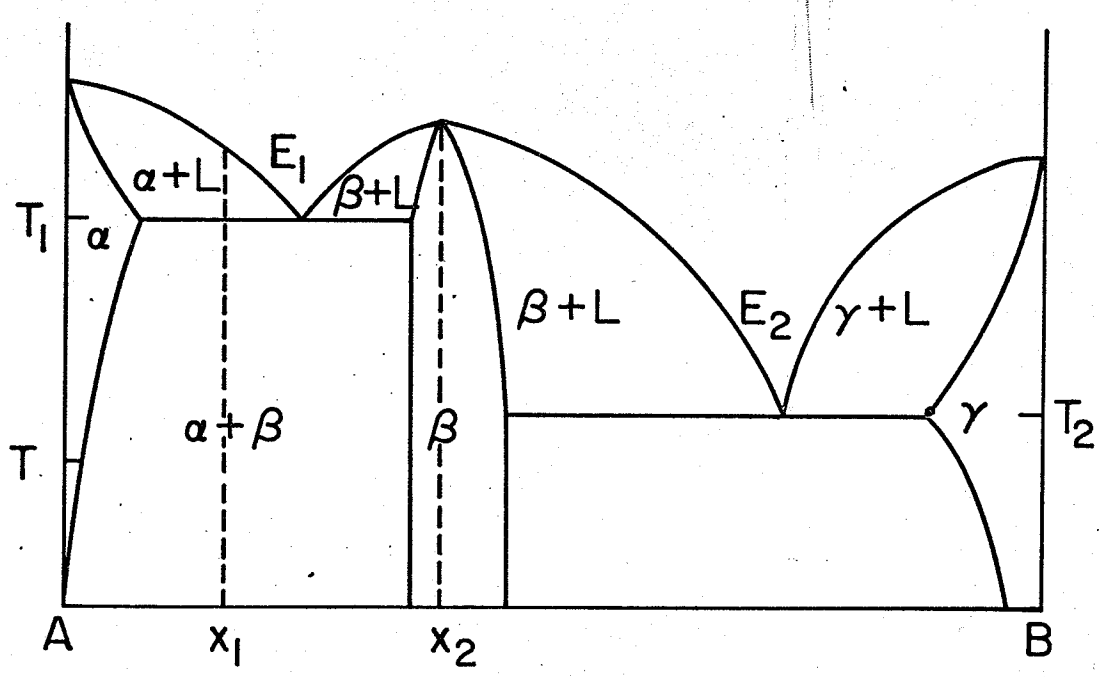

FIGURE 7 HYPOTHETICAL BINARY SYSTEM AB

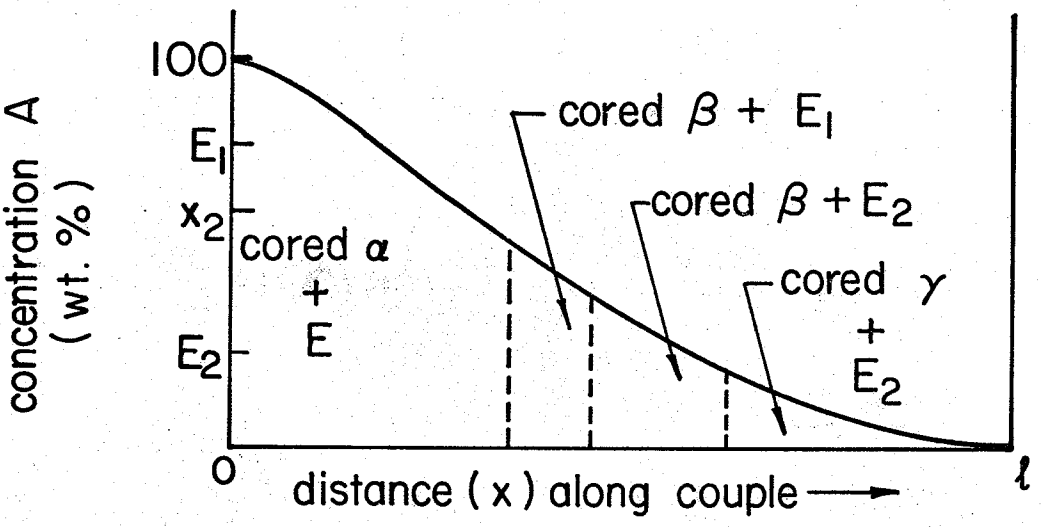

FIGURE 8a CONCENTRATION GRADIENT, AS SOLIDIFIED

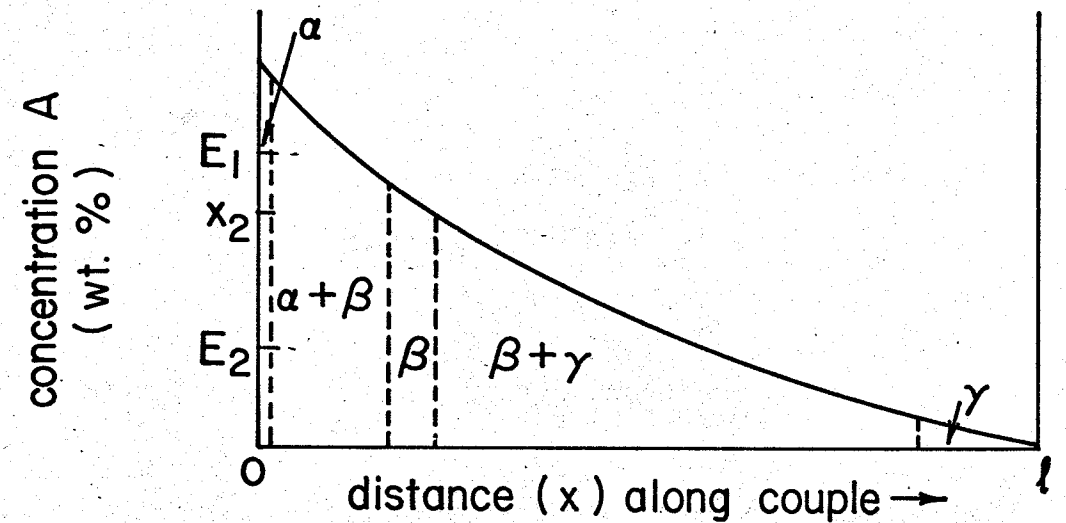

FIGURE 8b CONCENTRATION GRADIENT, HEAT TREATED AT T.

concentration gradient will result (Fig. 8b). There will be little mass transport along the length of the couple since solid state diffusion is comparatively slow but local equilibrium will be obtained. Consequently the equilibrium solid solubilities come into effect, coring is eliminated, and equilibrium phase relations result as depicted in figure 8b. This equilibrium can be done at any or all temperatures below T_2 with this couple to yield upon compositional analysis, the complete phase diagram. For the higher temperature section to the left of β, couples of β to A could be made to give the system up to T_1.

5.2 Ternary Systems

Both the ternary systems in Figure 9 display similar phase relations in the A (rich) end. To determine these phase relations a liquid diffusion couple could be made between the binary systems AC and AB at xx. Upon heat treatment, such a couple would yield the phase regions cut by xx. In order to determine which of the two ternary isothermal sections was correct, that is to determine whether γ is a binary or ternary compound, a diffusion couple could be made across the ternary system at yy. If system(9a) is representative then it will show some phase regions before the $\beta + \gamma$ region, as shown in Fig. 9b. If, however, system(9b) is representative, then the couple starts with the $\beta + \gamma$ region from the AC binary system end. This type of discrimination is necessary in ternary systems to determine whether phases are binary phases extended into the ternary diagram, or whether they are true ternary phases. In other respects, determining the ternary diagram is the same as for a binary system. Liquid diffusion couples could be made across the corners of the ternary system at compositions judged from the binary diagrams that make up the periphery of the ternary system.

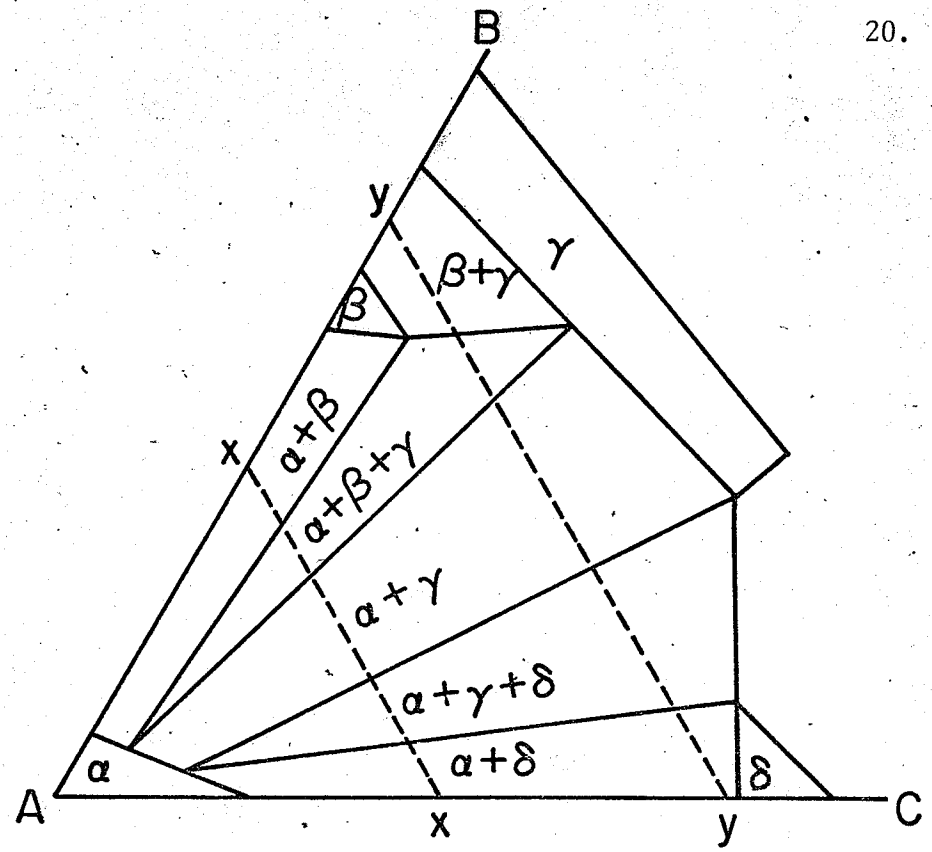

FIGURE 9a HYPOTHETICAL TERNARY SYSTEM ABC, CASE I

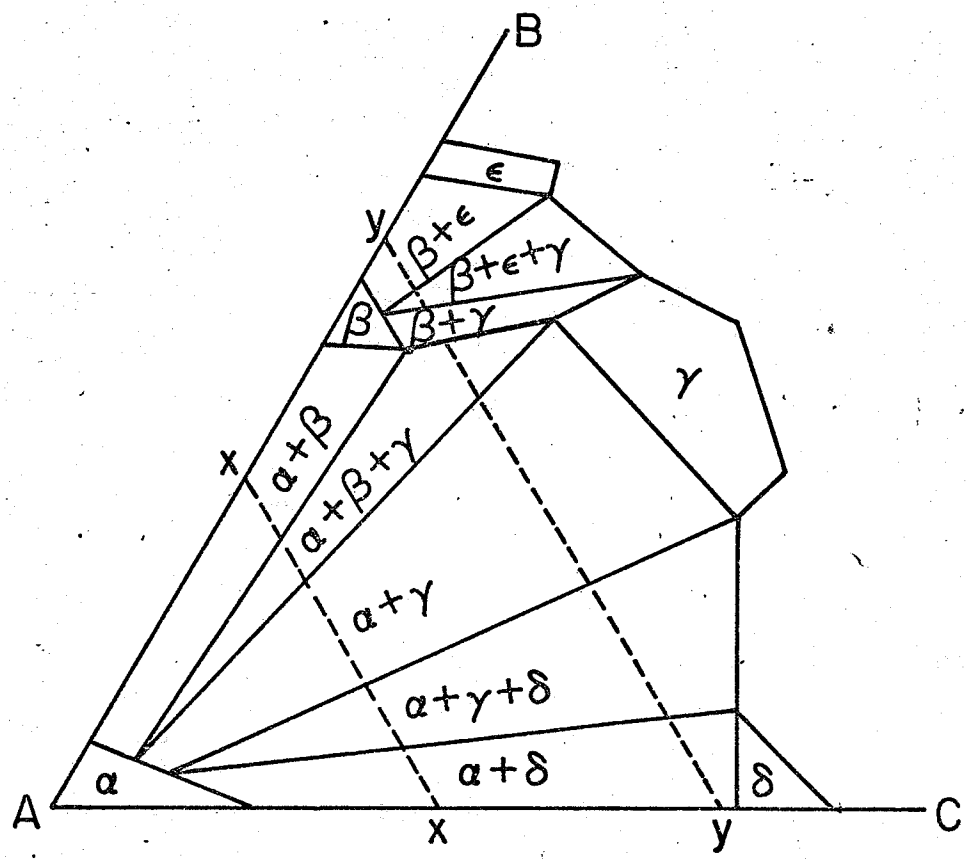

FIGURE 9b HYPOTHETICAL TERNARY SYSTEM ABC, CASE II

Systematic heat treatment of couples at different temperatures would again yield the complete diagram in terms of isothermal sections up to the lowest solidus temperature.

6. EXPERIMENTAL TECHNIQUES

6.1 Preparation of Diffusion Couples

6.1.1 Materials

The purity of the materials used was as follows-:

aluminum - 99.999%

copper - 99.96%

nickel - 99.9%

magnesium- 99.9%

6.1.2 Capillary Techniques

It was initially decided to use capillaries for the liquid diffusion technique to minimize convective mixing. The capillaries were constructed from 3/16" diameter graphite rod drilled with .9 mm. drill to a depth of 1" to 1 1/4". They were filled with metal (Al-18Ni, Al-23Cu, or pure Mg) in a specially constructed vertical tube vacuum furnace (fig. 10 a,b).

The capillaries were placed in a holder extending through the open end of the vacuum furnace. Holding the capillaries above the alloy with which they were to be filled, the top was placed on the furnace and the metal melted. In the case of magnesium the melting was done under an argon atmosphere. When the metal was molten, the furnace was evacuated and the capillaries lowered into the melt. For the magnesium melt, the evacuated time was held as short as possible since the magnesium vaporized

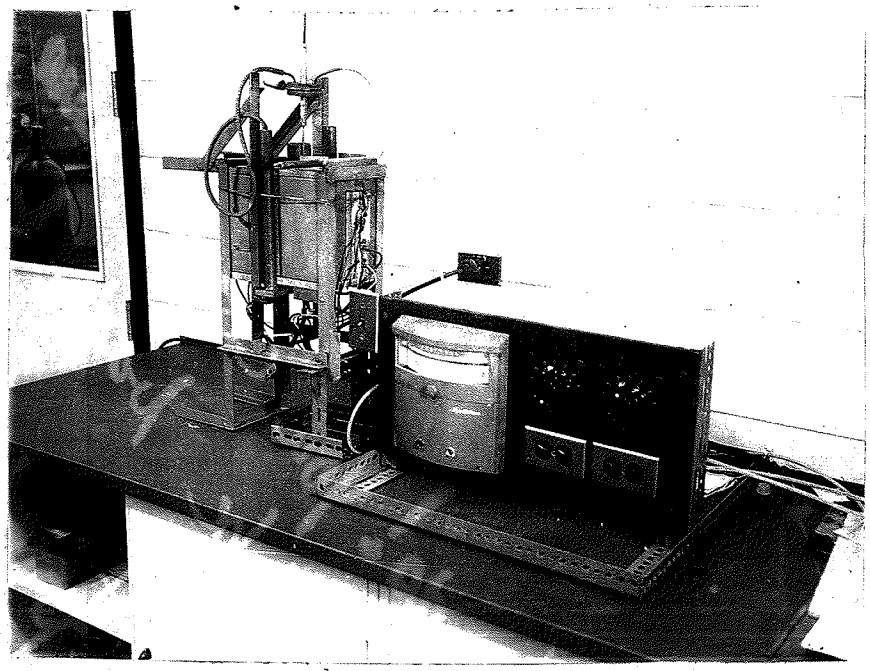

Figure 10a. Capillary Furnace

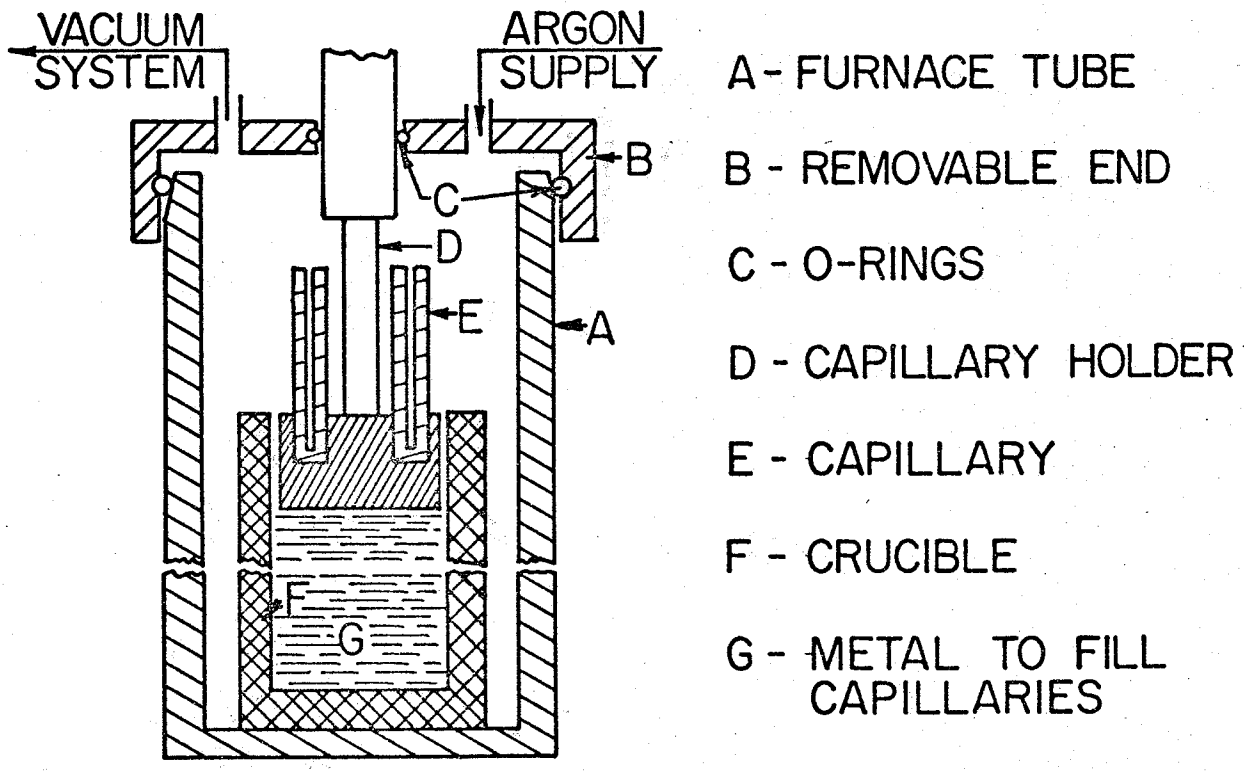

FIGURE 10b CAPILLARY FILLING FURNACE

very rapidly. After half a minute in the melt, air was allowed into the furnace (argon for Mg) forcing molten metal into the capillaries, and then the capillary holder was raised from the melt.

The capillaries were then faced off smoothly and placed horizontally (for Al-Cu or Al-Ni capillaries) or vertically (Al-Mg capillaries) (fig. 11) in a carbon rod. This rod was placed in molten alloy to allow liquid diffusion to occur. The times and temperatures for diffusion were experimentally determined to be 40 minutes for Al-23 Cu capillaries in Al-18Ni bath at 850°C and 25 minutes for a Mg capillary in an Al bath at 700°C.

6.1.3 Standard Size Diffusion Couples

Recent investigations concerning liquid diffusion in the Cu-Ni system (19) indicate that ordinary Boltzmann-Matano diffusion couples may be used with no apparent convective mixing. Since the capillary technique was cumbersome it was decided to try larger ordinary diffusion couples. Admittedly, Cu and Ni have similar densities and less convective mixing would be expected than in the Al-Mg system. However, it is desired only to obtain a continuous concentration gradient from one initial concentration to the other and the mode of transport is not important. The size chosen as standard for the diffusion couple was 3/8" diameter. This sized couple was large enough to be handled easily and also had a cross section large enough to be examined for homogeneity.

The molds were constructed from 1" diameter graphite rod with 3/8" holes drilled centrally. The two halves of the couples were made from Al-Ni and Al-Cu alloys cast into a 3/8" mold from the melt or

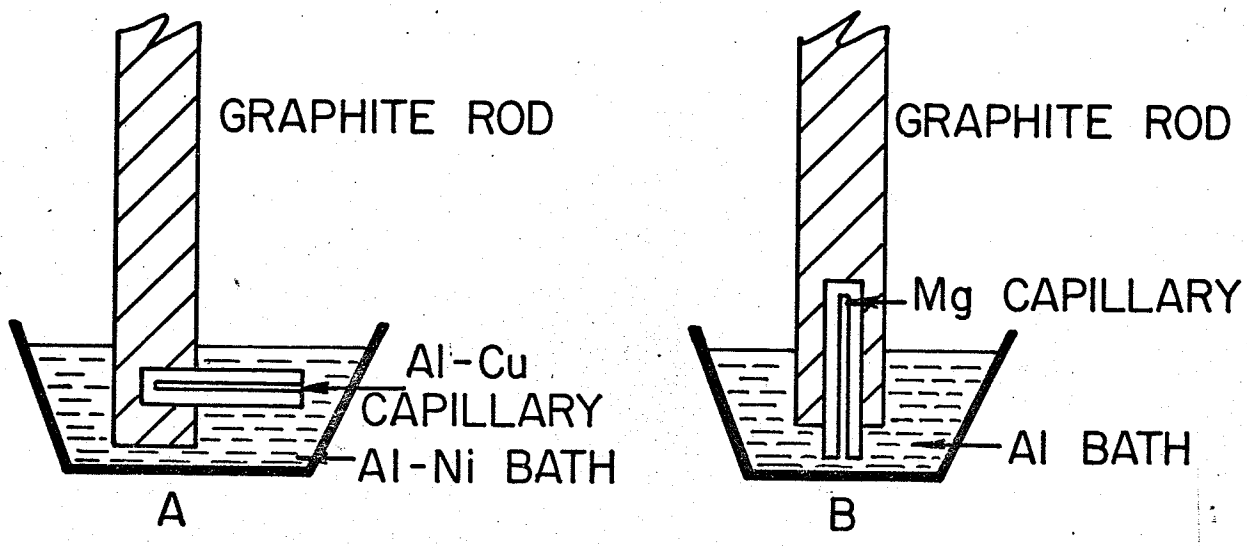

FIGURE 11 CAPILLARIES MOUNTED FOR DIFFUSION TO AVOID GRAVITATIONAL SEGREGATION

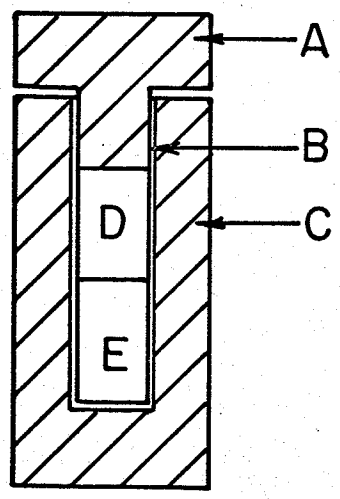

A - GRAPHITE CAP

B - ZrO_2 LINING

C - GRAPHITE CRUCIBLE

D,E - HALVES OF COUPLE

FIGURE 12 STANDARD 3/8" DIFFUSION COUPLE (actual size)

pure Al and Mg turned down from round stock to 3/8". Each half of the couple was about 1/2" long forming a Boltzman-Matano type diffusion couple 1" in length (fig. 12). After the end pieces for the couple had been placed in the mold, a graphite plug was placed in the open end. This provided both a token air seal, and served to press the two pieces of the couple together. The couple was then placed in a furnace for an experimentally determined time (about 20 minutes) at a temperature about 50°C above the liquidus of the metal. The Al-Mg couples were diffused under an argon atmosphere.

For high melting point alloys it was necessary to coat the molds with a zirconia slurry to avoid picking up carbon from the molds. Furthermore, the temperatures required for liquid diffusion were not attainable in resistance furnaces. Consequently the induction furnace was tried, but due to insufficient damping of induced currents homogeneous alloys, rather than diffusion couples, resulted. Finally adequate couples were made simply by heating with an oxy-acetelyne torch.

6.2 Heat Treatment

The Al-Mg couples were encapsuled in pyrex glass evacuated and flushed five times with argon and filled to a partial pressure of 350 mm. with argon. The couples were then heat treated for a week at 380°C, and water quenched. One couple was heat treated an additional week at 280°C.

The Al-Cu-Ni couples were not encapsuled in glass since aluminum alloys develop their own protective oxide layer. They were heat treated at 535°C for one to three weeks and then water quenched. The furnace controllers were accurate to ±1°C. After heat treatment

the couples were mounted in bakelite, sanded, and polished.

6.3 Optical Microscopy

All specimens were polished on #220 through #600 carborundum paper, then with 6 μ diamond paste, and finally with 0.3 μ aluminum oxide powder using water as a lapping medium.

The Al-Mg couples were etched with 20% HNO_3 and water for varying times depending upon the phases to be observed.

The Al-Cu-Ni couples were etched with Keller's etch for varying times from 5 to 20 seconds and with 20% HNO_3 in water for 5 seconds depending upon the phase to be observed.

The micro-hardness of all phases was also determined in order that this could be used as a distinguishing factor between phases.

All specimens were examined and photographed in the as cast and heat treated conditions at various magnifications from 5 to 1350 times.

6.4 Electron Probe Microanalysis

All couples were prepared for electron probe analysis by polishing to 0.3 μ aluminum oxide powder. The Al-Cu-Ni couples were etched for 2 seconds in 20% HNO_3, 2% HF, the remainder water, and the Al-Mg couples were etched for 5 seconds in 20% HNO_3.

For the Al-Mg couples a Materials Analysis Corporation (MAC5) probe with a take off angle of 38.5° and an incident electron beam angle of 60° was used. A standard of pure aluminum was used and the $K_{\alpha 1}$ radiation from aluminum was monitored.

Two types of analysis were done. One involved a large beam diameter used to take average readings in the area of phase boundaries.

The other utilized a small beam diameter to measure composition of individual phases in two or three phase regions. Two couples, one covering the whole Al-Mg system, the other just the region from β to γ were analyzed.

For the Al-Cu-Ni system a Phillips AMR/3 electron probe micro-analyzer with take-off angle of 15° was used. Cu and Ni concentrations were determined using the phases in the couples themselves as standards: - ε (Al-42 wt% Ni), with a stoichiometric formula of Al_3Ni, for nickel, and θ (Al-52 wt% Cu), with a formula centering on Cu Al_2, for copper. The elements were standardized, on the $K_{\alpha 1}$ peaks, at the high nickel and high copper ends respectively. The composition of each phase was determined in each phase region using a beam of about one micron diameter. Five counts of ten second duration were taken of copper and nickel at each spot and averaged. The average composition of the place where readings were taken was also determined. In two phase regions, analysis was generally done both in the middle of the region and near the boundaries of the adjacent three phase zones.

7 RESULTS AND DISCUSSION

The capillary technique for producing the liquid diffusion couples, which was adopted to prevent convection from being the material transport mechanism, was found to be unnecessary. The capillaries, made of graphite, were found to be awkward to handle, delicate and subject to breakage, difficult to mount for examination, and quite difficult to fill with reactive material such as magnesium. However, concentration gradients and different phase fields were evident in the capillaries indicating the

feasibility of the method.

Larger couples (3/8" diameter) were consequently adopted and found to be suitable. Undoubtedly there is some convective mixing. The con centration profiles were too extended for the short diffusion times if diffusion was indeed the only transport mechanism. This can be seen if one considers that individual atoms had travelled up to 1/2" in diffusion times of about 20 minutes. Also couples made with different diffusion times (20 minutes, one hour, two hours) showed little difference in the length of the diffusion zone. Hence it was concluded that some convection occurred right at the time of melting, providing most of the mass transfer, and then the concentration gradient was smoothed out by liquid diffusion. For couples made of similar melting point materials (Al-mp = 660°C, Mg-mp = 650°C), the convection was not sufficient to destroy the concentration gradient (fig. 13) and the phase boundaries were straight parallel lines running across the couple (fig. 14). Boundaries were not perpendicular to the sides of the couple due to the difficulty in placing the couple perfectly upright in the small vacuum furnace.

7.1 Al-Mg System

The as-cast Al-Mg couple was examined and found to contain the same number of phases, and phase reactions as indicated by Hansen (10). Hence the phases were tentatively identified as α, β, γ and δ in order of their appearance from the Al rich end of the couple. Under the 20% HNO_3 etch the magnesium end was attacked readily while a longer time was required to bring out the distinction between α and β, and β and γ. The Al (rich) end, or α appeared white after etching, β brownish, γ white tending to a darker greyish tint, and pure δ was also whitish. The main

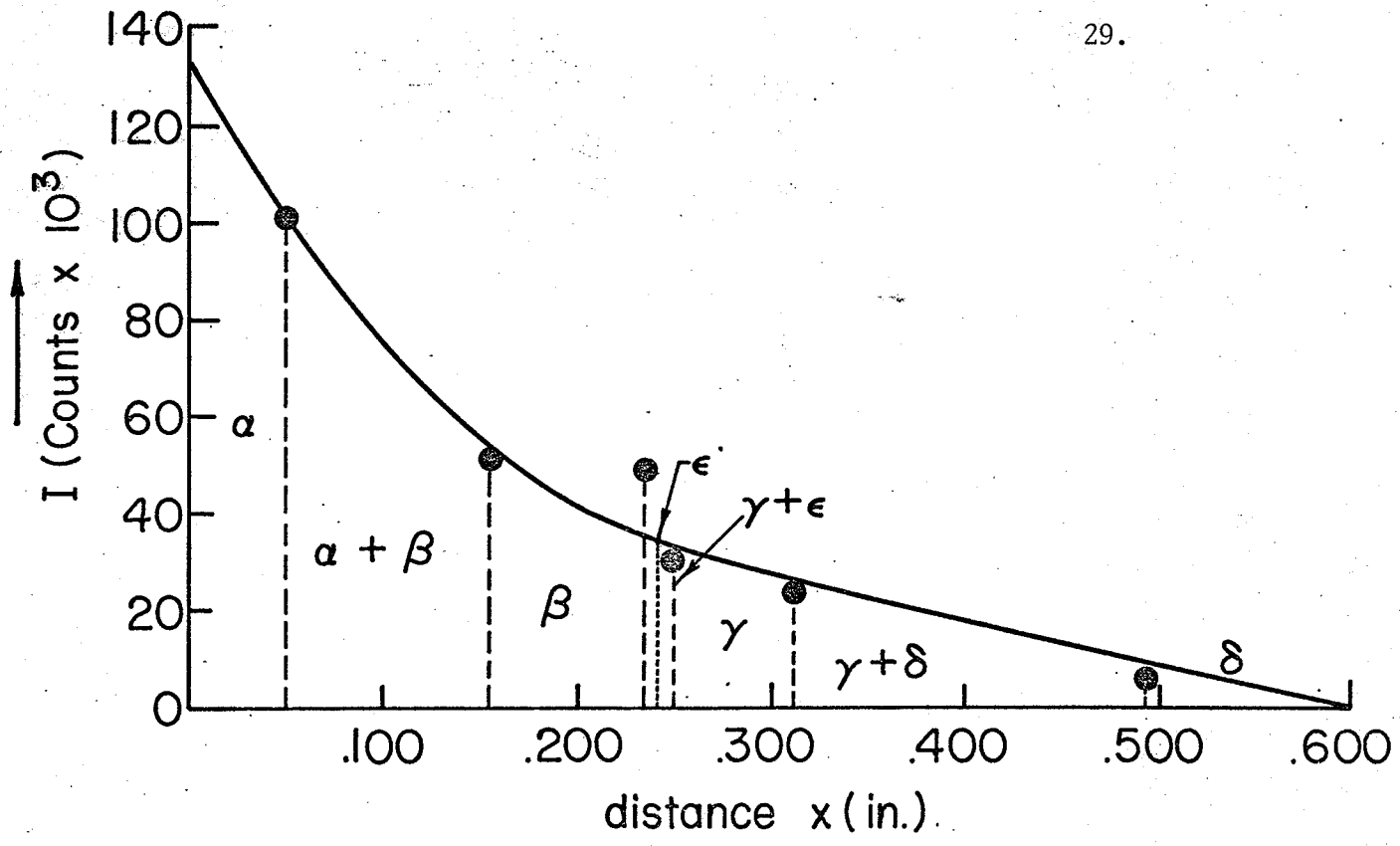

FIGURE 13 INTENSITY VS DISTANCE ALONG COUPLE FOR HEAT-TREATED Al-Mg DIFFUSION COUPLE

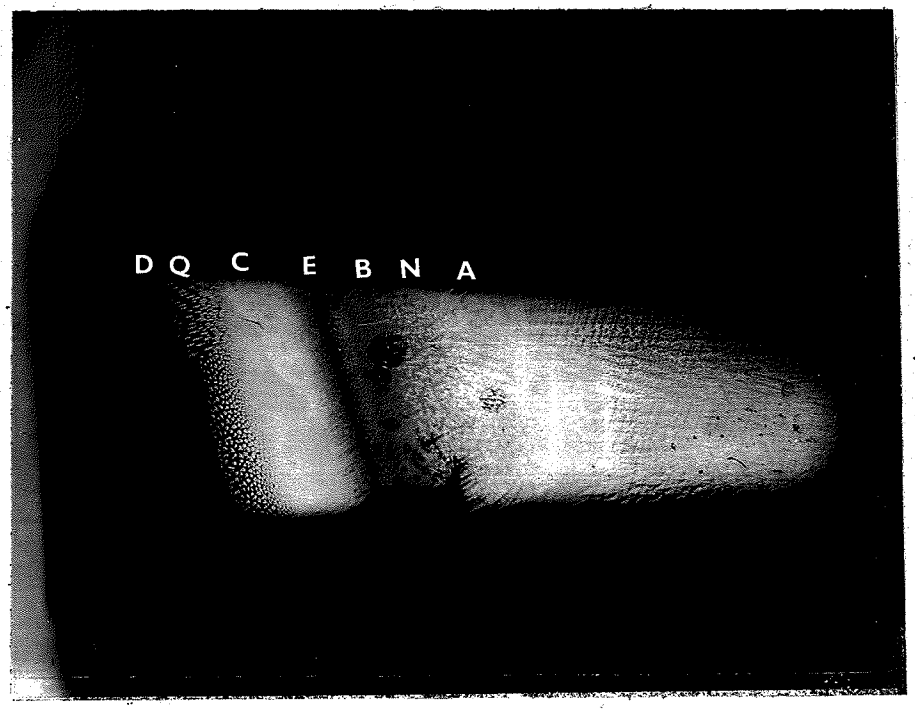

D = δ region
Q = δ+γ
C = γ
E = β+γ
B = β
N = α+β
A = α

Figure 14. Al-Mg Couple, as-cast, etched 5 sec. in 20% HNO_3, 65x

distinguishing factor between α,γ andδ, being that all were etched much the same colour, was their order of appearance in the couple. Further, the pure α was hard to polish and was quite scratched, γ was hard and brittle and well polished, δ exhibited twinning and what appeared to be pitting.

Two eutectics as shown by Hansen (10) were evident in the couple - $\beta+\gamma$, $\gamma+\delta$ (fig. 15). The $\alpha+\beta$ eutectic contained too little α to be distinquished. The $\alpha+\beta$, β, $\beta+\gamma$, γ, and$\gamma+\delta$ regions are shown in figures 16a-e. These results indicate the general nature of the liquid → solid reactions in the Al-Mg system and the phase fields present are identical to those expected from the phase diagram (10).

After observation of the as cast structure, the diffusion couple was heat treated for one week at 380°C, then quenched in water. The phase fields present in the couple, α, $\alpha+\beta$, β, ε, $\varepsilon+\gamma$, γ, $\gamma+\delta$, δ are shown except for α and δ in figs. 17a-f. The $\varepsilon+\beta$phase field is not present. The kinetics of formation of ε are likely sluggish, however, as evidenced by the uncertainty of its existence (10) and therefore it is probably that the one week heat treatment at 380°C was insufficient to establish complete equilibrium.

Two types of probe analysis were performed on the Al-Mg couples. One was large beam diameter probing to determine the concentration gradient; the other a small spot analysis of the phases in the two phase regions to establish more exact compositioned phase boundaries. Using the large beam diameter, the average concentration of Al was determined at various points along the length of the diffusion couple and the positions of the phase field boundaries were established along the concentration gradient. The

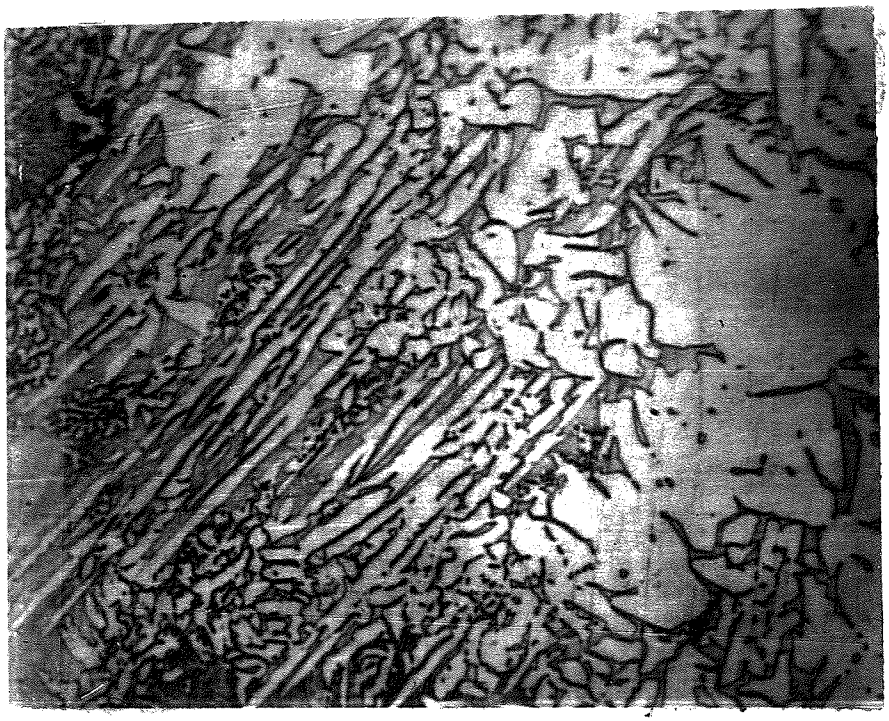

light region is β

dark needles are γ

Figure 15a. β+γ region in as-cast Al-Mg couple, etched 5 sec. in 20% HNO_3, 450x

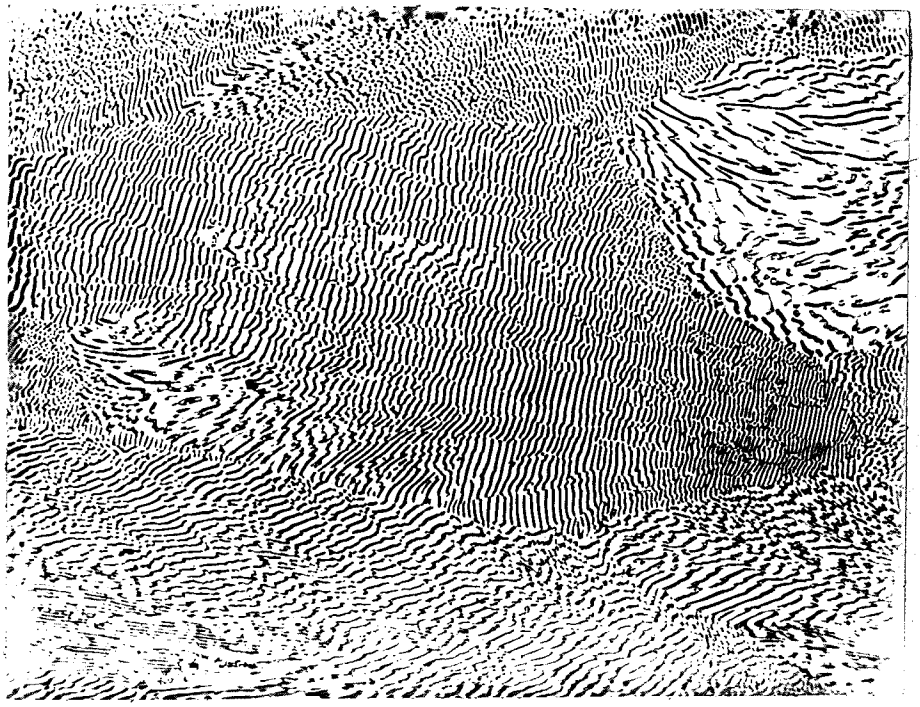

light lamellae = δ

dark lamellae = γ

Figure 15b. γ+δ eutectic, as-cast Al-Mg couple, etched one sec. in 20% HNO_3, 800x

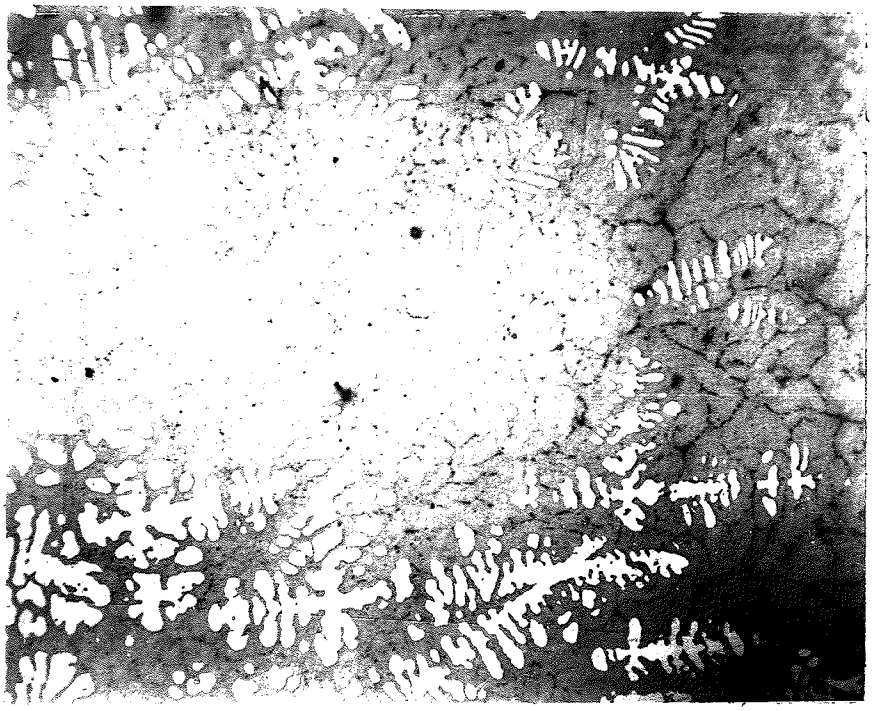

Figure 16a. α+β region, as-cast Al-Mg couple, etched 10 sec. in 20% HNO_3, A = α, B = β, 85x.

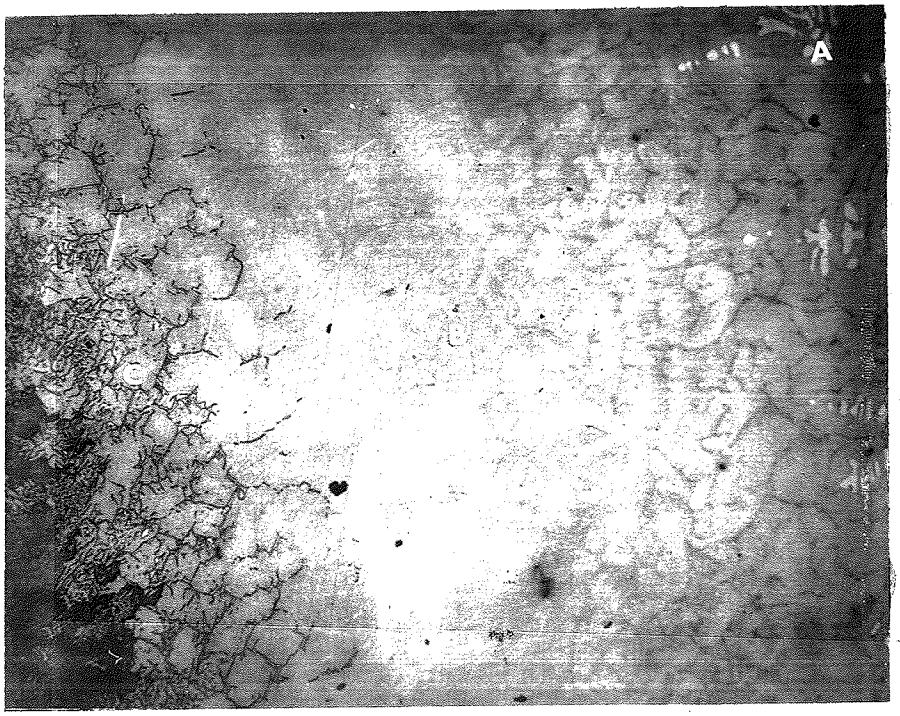

Figure 16b. β region, as-cast Al-Mg couple, etched 10 sec. in 20% HNO_3. A = α, B = β, C = β+γ, 85x

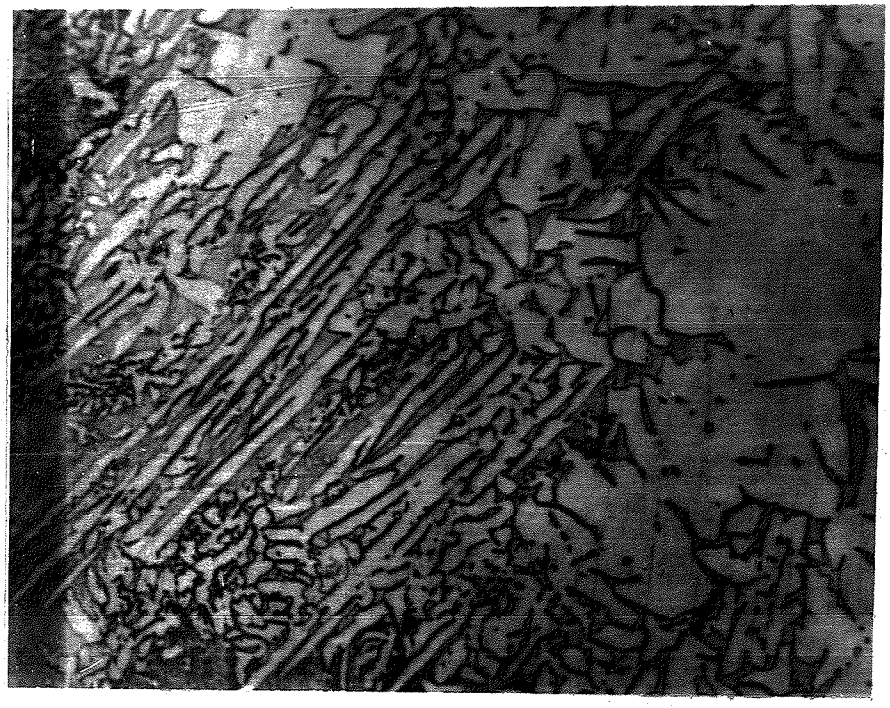

light region is β

dark needles are γ

Figure 16c. β+γ region, as cast Al-Mg couple, etched 10 secs. in 20% HNO_3, 450x

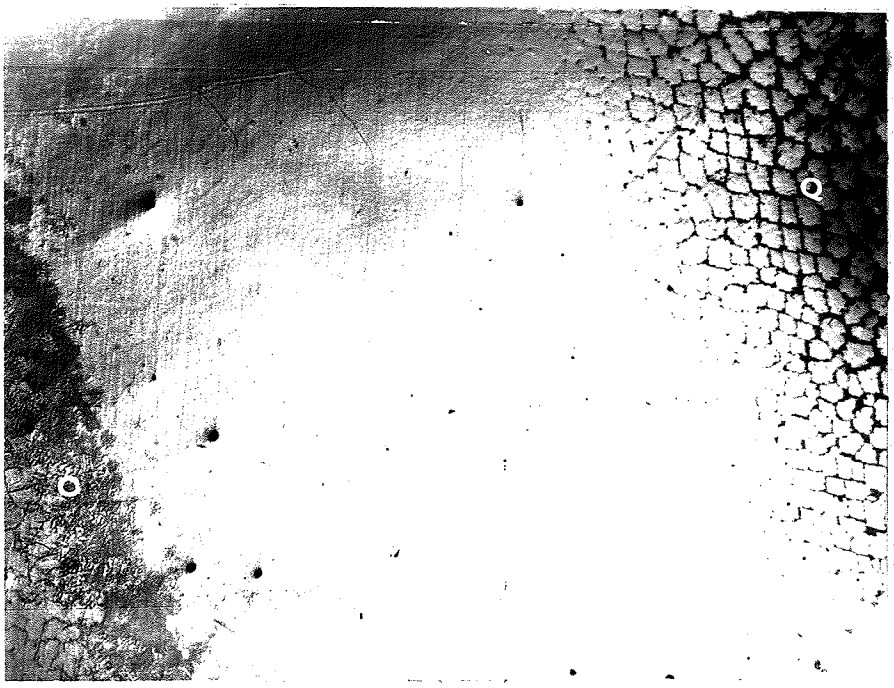

Figure 16d. γ region, as cast Al-Mg couple, etched 10 secs. in 20%HNO_3

O=β+γ, C=γ, Q=γ+δ, 42x.

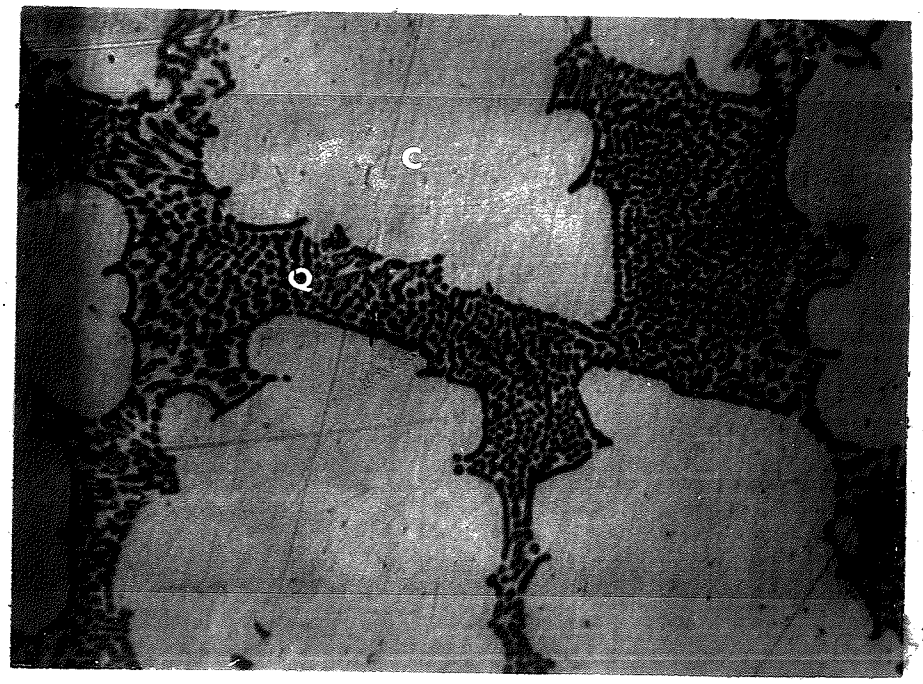

Figure 16e. $\gamma+\delta$ region, as-cast Al-Mg couple, etched 2 secs. in 20% HNO_3, Q = $\gamma+\delta$ eutectic, c = γ, 800x

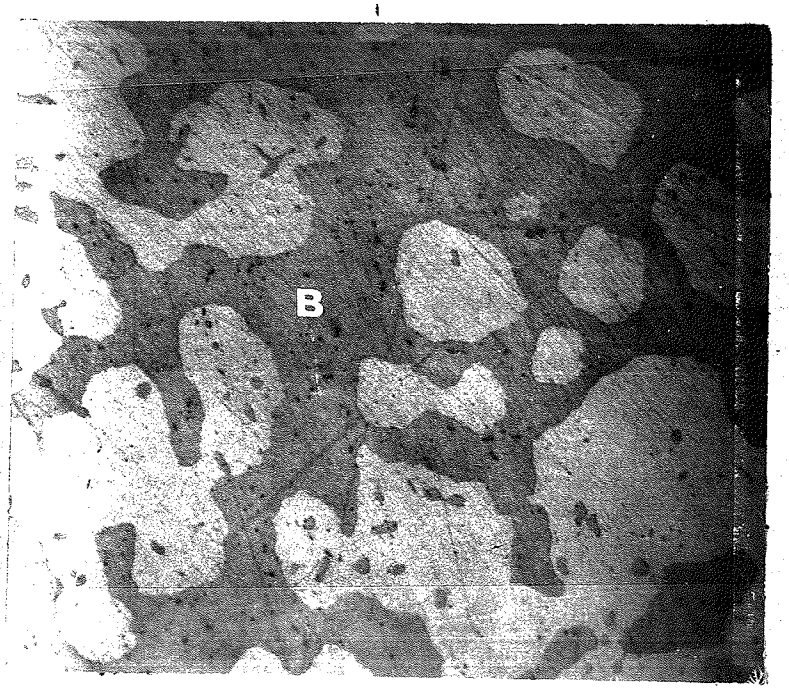

Figure 17a. $\alpha+\beta$ region, heat treated Al-Mg couple, etched 10 seconds in 20% HNO_3 A = α, B = β, 800x

Figure 17b. β region, heat treated Al-Mg couple, etched 10 secs. 20% HNO_3, A = α, B = β, 85x

Figure 17c. ε and ε+γ region, heat treated Al-Mg couple, etched 5 secs. in 20% HNO_3, B = β, E = ε, C =γ, region between E and C is ε+γ , 350x

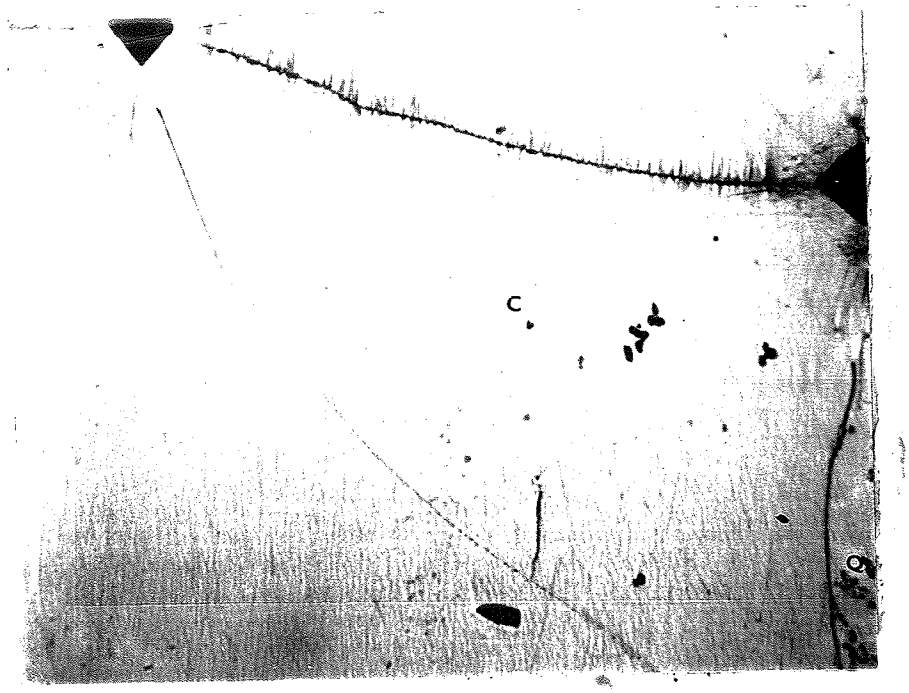

Figure 17d. γ region, heat treated Al-Mg couple, etched 5 secs. in 20% HNO_3, Q = $\gamma+\delta$, C = γ region (between hardness indentations), 85x.

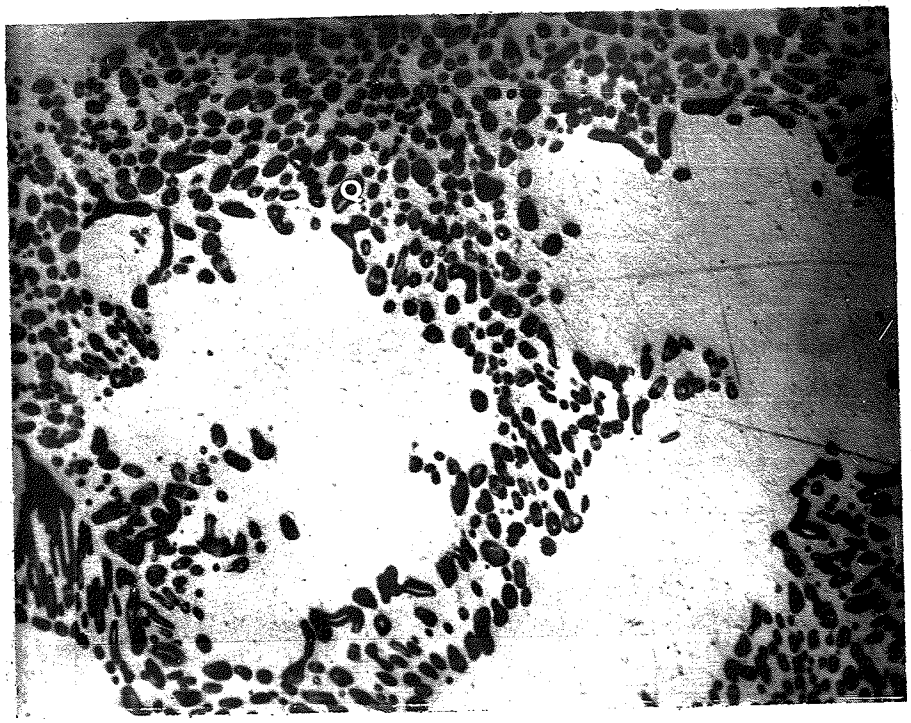

Figure 17e. $\gamma+\delta$ region, heat treated Al-Mg couple, etched 2 secs. in 20% HNO_3, Q = $\gamma+\delta$ eutectic, C = γ, 600x.

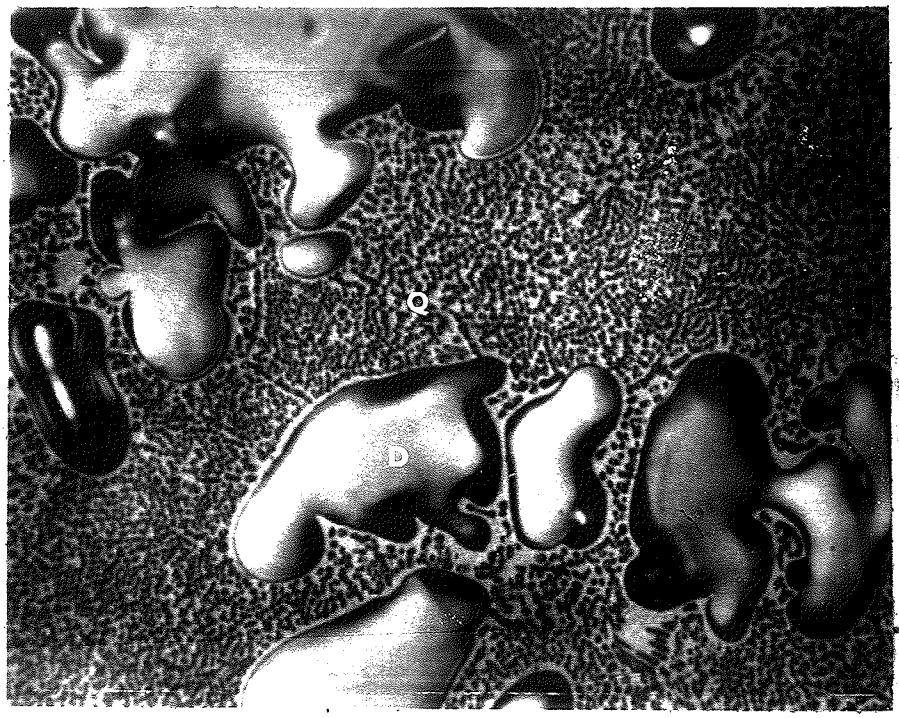

Figure 17f. $\gamma+\delta$ region, heat treated Al-Mg couple, etched 2 secs. in 20% HNO_3, Q = $\gamma+\delta$ eutectic, D = δ, 600x.

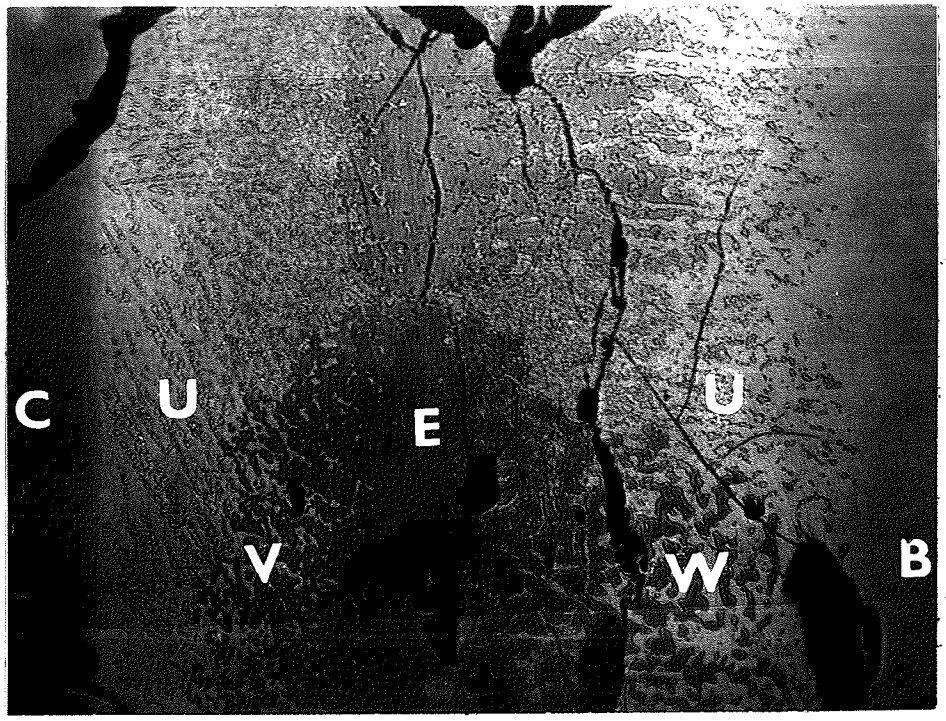

C = γ region
U = $\beta+\gamma$
V = $\varepsilon+\gamma$
E = ε
W = $\varepsilon+\beta$
U = $\beta+\gamma$
B = β

Figure 18. ε region, heat treated Al-42%Mg couple, etched 5 secs. in 20%HNO_3, 30x

result is an isothermal section for the Al-Mg system at 380°C, which may be taken off figure 13.

More exact compositional boundaries of the phase fields were determined from analysis of the individual phases in two phase regions. This is valid since the compositions (in equilibrium) of the phases in a two phase region is that of the boundaries between the one and two phase regions. Thus from the $\alpha+\beta$ region, the high Mg boundary of the α region and the high Al boundary of the β region may be established. Similarly results were obtained for the other two-phase regions. A summary of the results of this analysis is given in table I and compared with those given by Hansen (10).

TABLE I Compositions of the phase field boundaries in the Al-Mg System.

Phase Field	$\alpha + \beta$		$\varepsilon + \gamma$		$\gamma + \delta$	
Phase	α	β	ε	γ	γ	δ
Hansen (10)	88*	64	58	53	41	10
Author's	90.5	64	60	54	42	12.5

No results are given for the $\beta+\varepsilon$ region since this phase field was not present in the diffusion couple.

A more complete analysis is given in the appendix, table VI

To establish more accurately the composition limits of the ε phase, another couple with the lengths of Al and Mg adjusted to give an

---

* All compositions given in wt % Aluminum

average composition of 42% Mg (the composition of the ε phase) was made. This couple was diffused two hours at 700°C in an attempt to decrease the concentration gradient through the ε composition and thus enlarge the ε region in the couple. After diffusion, the couple was heat treated for one week at 380°C then quenched in water. The phase fields, present as determined by probe analysis, were β, β+γ, β+ε, ε, ε+γ, β+δ, and γ with the ε, ε+β, ε, and ε+γ fields between two β+γ fields (figs. 18). This was at first confusing but is actually quite reasonable since the ε phase transforms from the γ+β field (10).

Table II Compositions of ε in the Al-Mg System

Phase Field	β	γ	β + γ	
Phase	β	γ	ε near γ	ε near β
Authors	63 (std)	52.5%	60.5	58.5
Hansen (10)	63	53	59	57

The biggest problem with doing probe analysis in the Al-Mg system is that of absorption correction. The great variance in absorption correction factors $-\mu_{MgAl} = 4300$ vs $\mu_{AlAl} \doteq 300$ makes the choice of assumed composition very critical. It is difficult to produce exact values using only pure metals as standards in any case since the tables for absorption correction are only accurate within 5% (3).

7.2 Al-Cu-Ni Ternary System

The Al-Cu-Ni ternary system was initially studied using a liquid diffusion couple with a gradient from Al-18%Ni to Al-23%Cu. The couple was diffused at 700°C for 20 minutes then allowed to cool slowly. Inspection of the as-cast structure reveals considerable information concerning the liquid solid reactions but the analysis is somewhat more complicated than in a binary system and is therefore discussed later, 7.3. After the analysis of the as-cast structure the couple was heat treated for

three weeks at 535°C, then quenched in water. The phase fields present after heat treatment were $\kappa+\varepsilon$, $\kappa+\varepsilon+\chi$, $\kappa+\chi$, $\kappa+\chi+\theta$, and $\kappa+\theta$, shown in fig. 19a-c, where χ is an unknown phase. From previous investigation (2) (4) it would appear that the unknown phase is either δ, a ternary extension of the binary phase Al_3Ni_2, or τ, a compound existing only in ternary alloys. To determine the nature of the unknown phase a diffusion couple was made with a concentration gradient from Al-50%Ni to Al-33%Cu. Al-50%Ni lies in the $\varepsilon+\delta$ region and therefore if the unknown phase is a ternary extension of the binary δ the phase fields in the couple should be, in order of their appearance from the Ni rich end, $\varepsilon+\delta$, $\varepsilon+\delta+\kappa$, $\delta+\kappa$, $\kappa+\delta+\theta$, $\kappa+\theta$. If the unknown phase is a pure ternary compound the phase fields should be $\varepsilon+\delta$, $\varepsilon+\delta+\chi$, $\varepsilon+\chi$, $\varepsilon+\kappa+\chi$, $\kappa+\chi$, $\kappa+\chi+\theta$, and $\kappa+\theta$ (similar to fig. 9b.)

Initially, the Al-50%Ni alloy for the diffusion couple was prepared in an untreated graphite crucible. However, an extraneous phase appeared in the binary alloy in the form of long needles as shown in fig. 20a. It was suspected that the needles were carbides and therefore the graphite crucible was coated with a ZrO_2 slurry before melting. The coating virtually eliminated the needles (as shown in fig. 20b) and it was therefore concluded that the extraneous phase was indeed a carbide.

Since the $\varepsilon+\delta$ alloy has a high melting point (1400°C) the diffusion couples could not be made in resistance furnaces. An attempt was made to diffuse the couples in an induction furnace using a thick graphite container as a susceptor. However some currents were still induced in the couple itself and the result was a homogeneous couple with no concentration gradient.

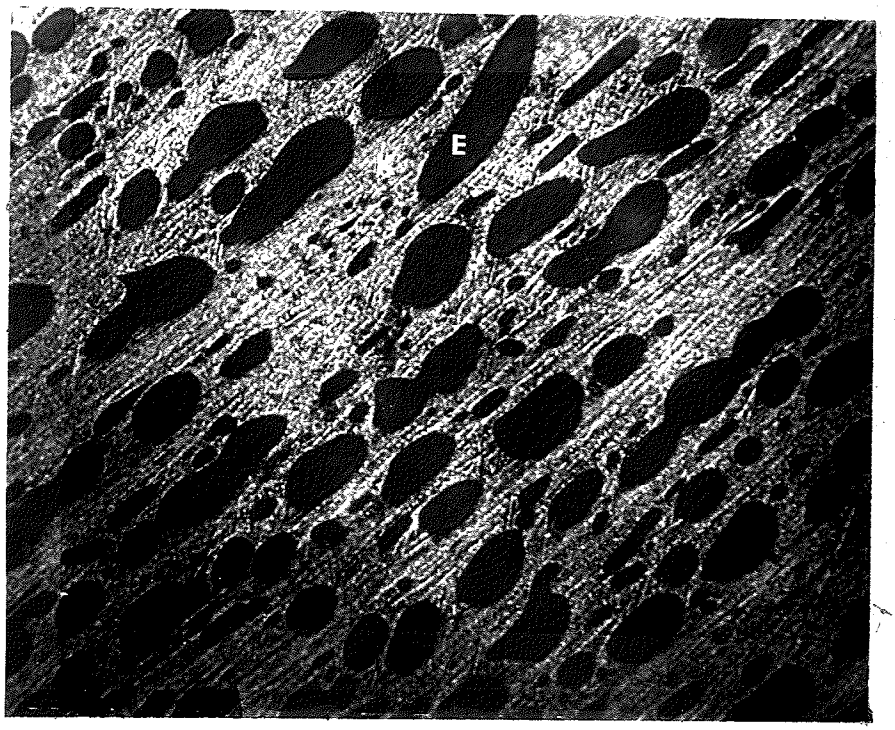

Figure 19a. κ+ε region, heat treated Al-18Ni to Al-23Cu couple, etched 3 secs. in Keller's etch, K = κ, E = ε, 500x

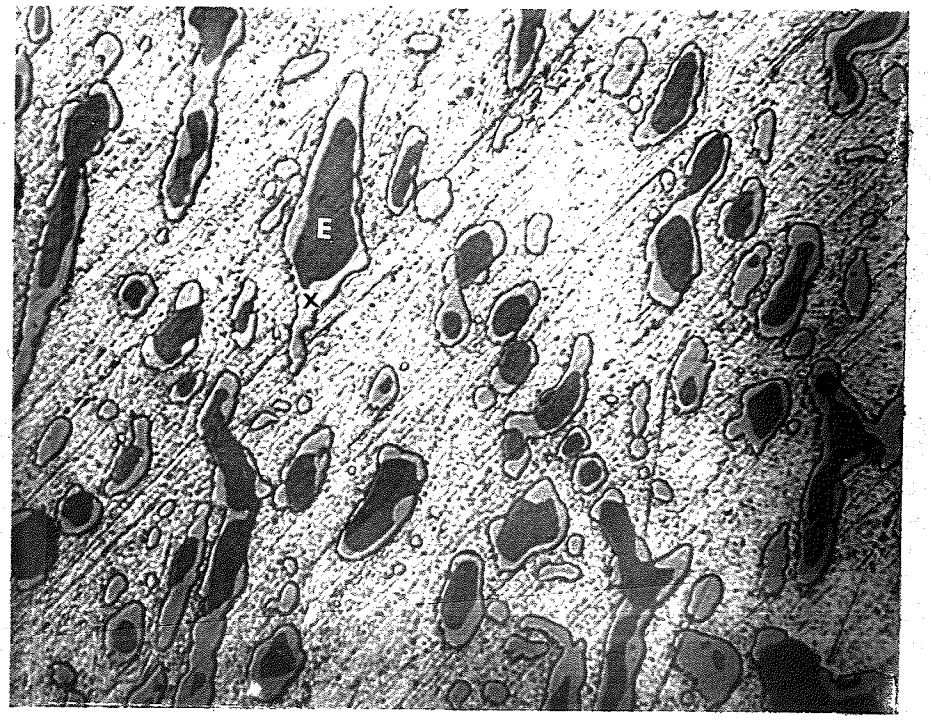

Figure 19b. κ+ε+χ region, heat treated Al-18Ni to Al-23Cu couple, etched 3 secs. in Keller's etch, E = ε, K = κ, X = χ, 500x

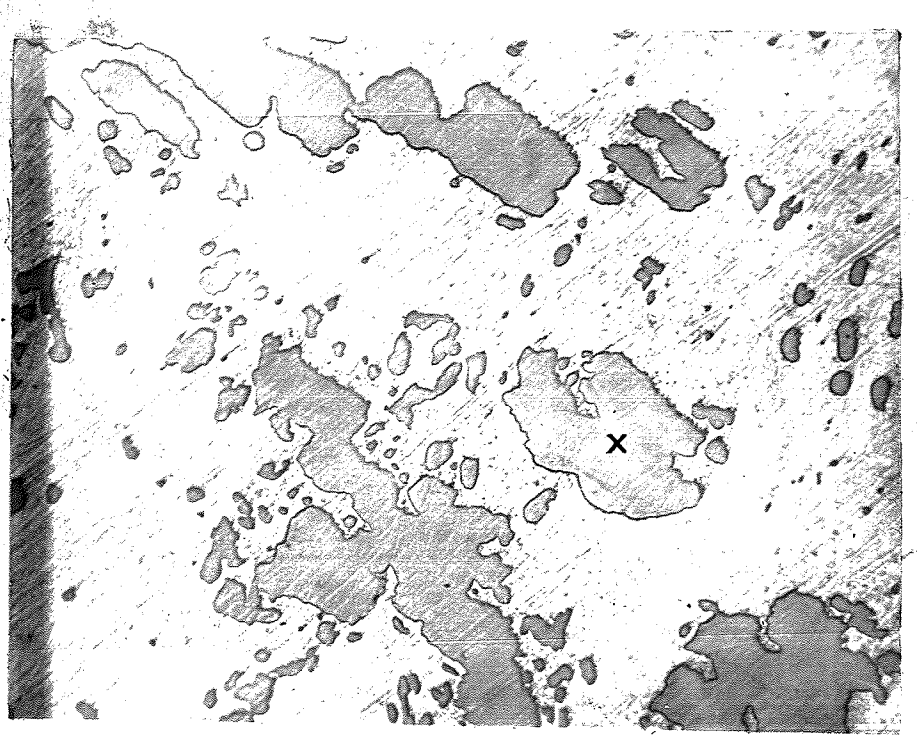

Figure 19c. κ+χ region, heat treated Al-18Ni to Al-23Cu couple etched 3 secs. in Keller's etch, X = χ, K = κ, 500x

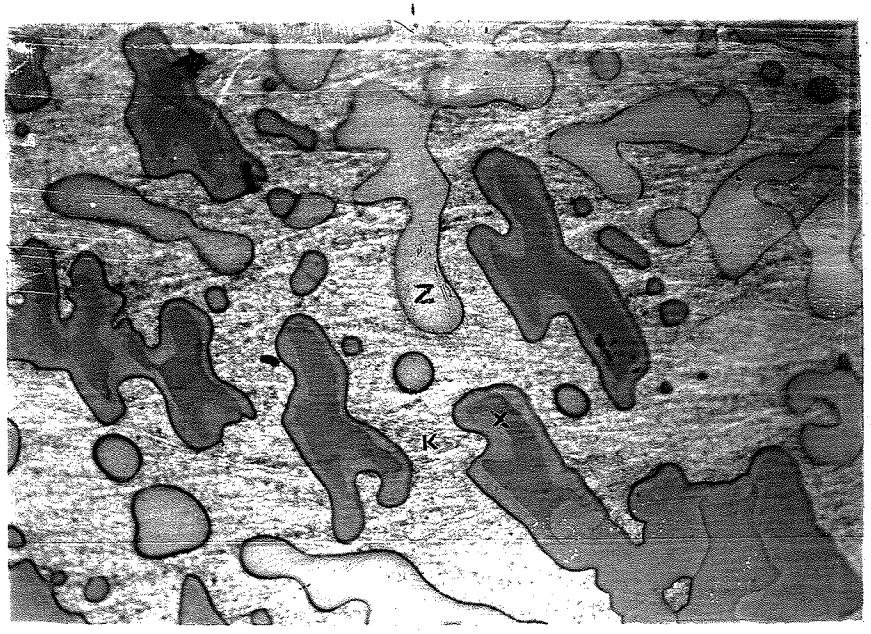

Figure 19d. κ+θ+χ region, heat treated Al-18Ni to Al-23Cu couple, etched 3 secs. in Keller's etch, K = κ, X = χ, Z = θ, 500x

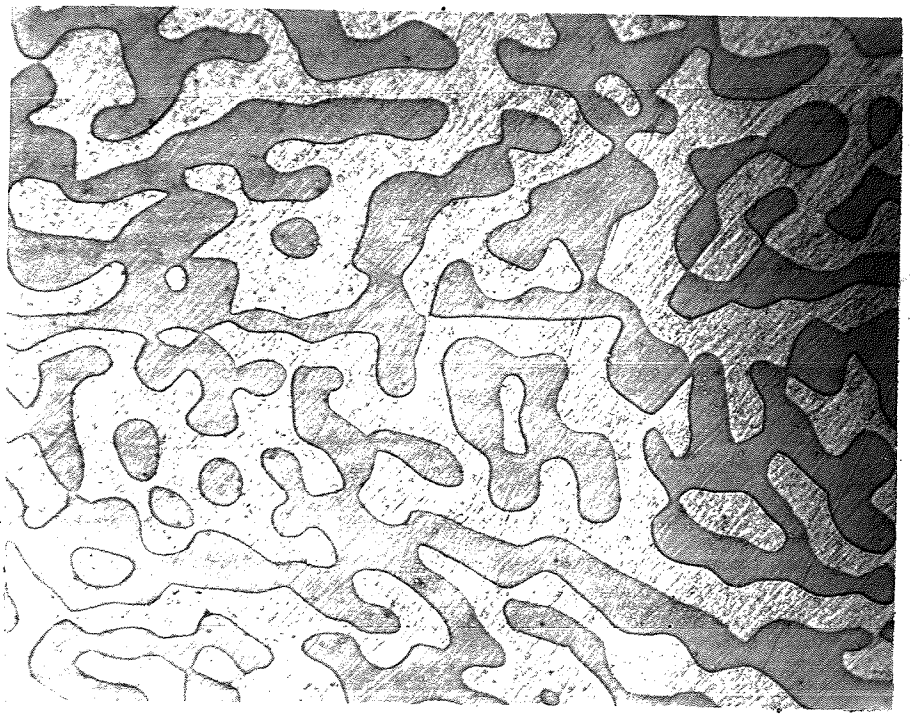

Figure 19e. $\kappa+\theta$ region, heat treated Al-18Ni to Al-23Cu couple, etched 3 secs. in Keller's etch, K = κ, Z = θ, 500x

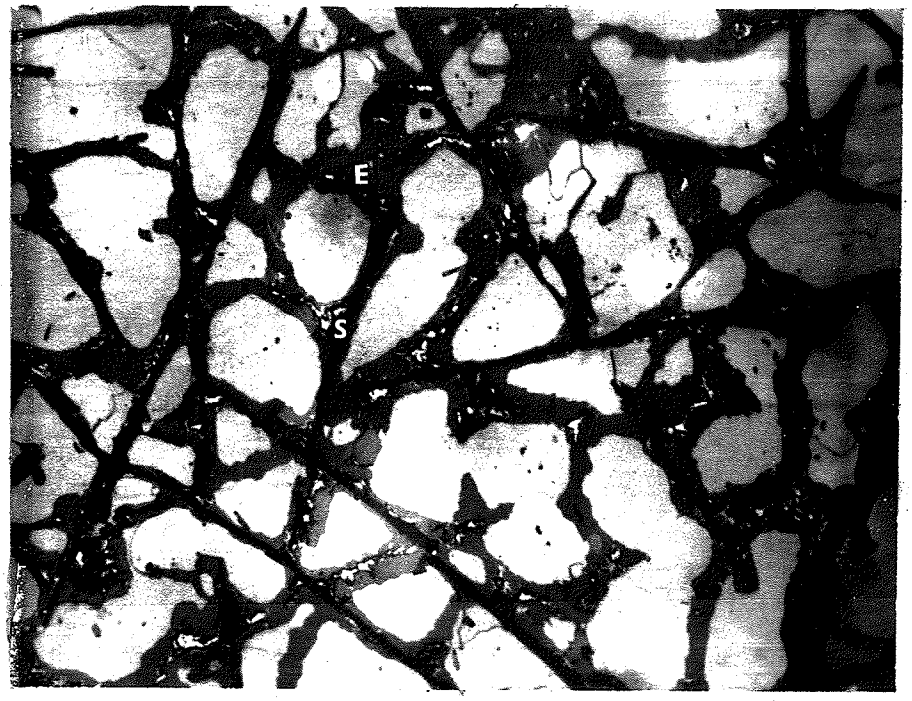

Figure 20a. $\varepsilon+\delta$ with carbide needles, etched 3 secs. in Keller's etch, D = δ, E = ε, S = carbide needle, 300x

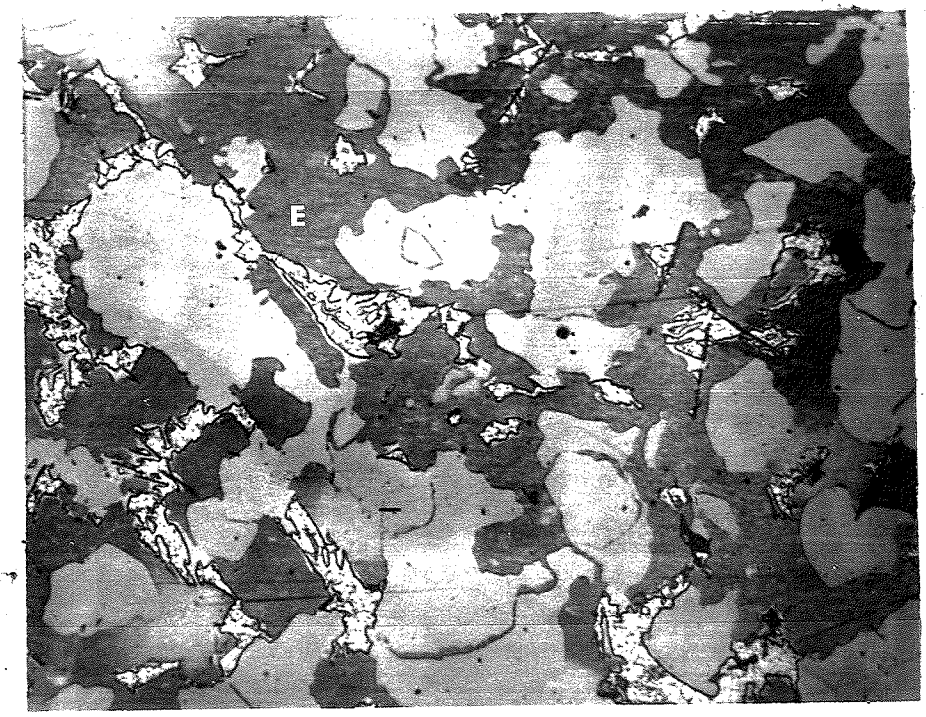

Figure 20b. κ+δ+ε with few carbide needles, etched 3 secs. in Keller's etch, D = δ, E = ε, K = κ, 500x

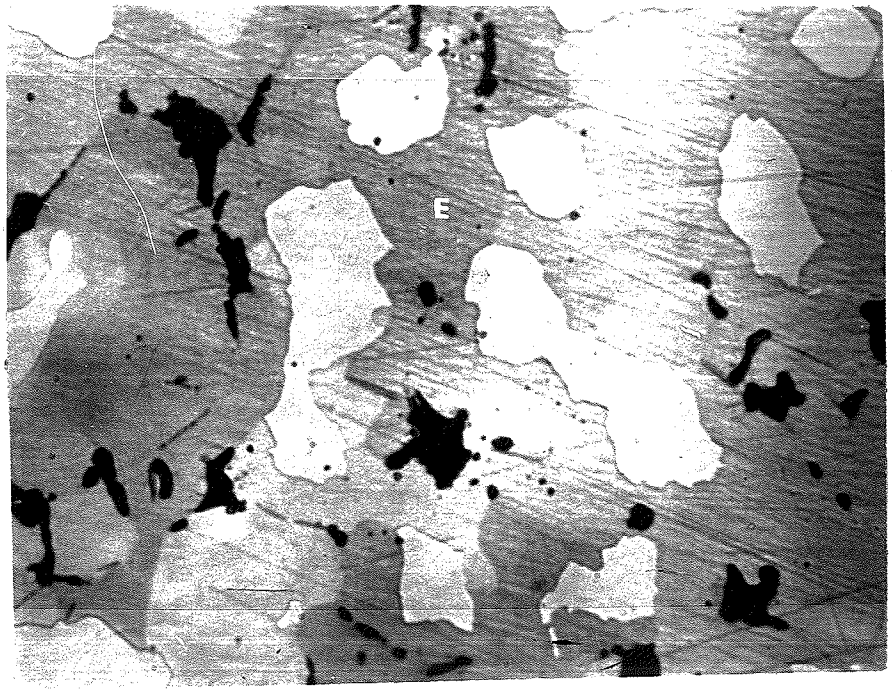

Figure 21a. δ+ε region, heat treated Al-50Ni to Al-33Cu couple, etched 3 secs. in Keller's etch, D = δ, E = ε, black spots are porosity, 780x

The diffusion couples were finally made successfully and simply by placing the end pieces of the couple in a ZrO_2 coated graphite mold and heating with an oxy-acetylene torch for about 15 minutes. Since the Al-50Ni alloy has a much higher melting point than the Al-33%Cu alloy (1400°C compared to 548°C) it was found that the Ni rich end of the couple had a concentration gradient from binary $\varepsilon+\delta$ whereas the Cu (rich) end appeared homogeneous and did not extend to $\kappa+\theta$. The homogeneity was likely a result of the low melting point alloy being molten considerably longer than the higher melting point alloy. The concentration gradient was extended to the binary $\kappa+\theta$ simply by cutting the homogeneous portion from the couple and making a second couple with this cut portion and a piece of Al-33%Cu alloy.

The phase fields in these two couples in order of their appearance from the Ni rich end were $\varepsilon+\delta$, $\varepsilon+\kappa+\delta$, $\kappa+\delta$, $\kappa+\delta+\theta$, and $\kappa+\theta$ shown in fig. 21 a-e. Therefore it was concluded that the unknown phase was δ. It is also clear that a pure ternary compound does not exist in the Al(rich) end of the Al-Cu-Ni ternary diagram.

A shading phenomena in δ (fig. 21c) did give rise to the possibility of another phase being present. Since δ has such a large phase field, varying in both composition and presumably solidus temperature, the shading was considered to be a result of coring. The short heat treatment time afforded the high alloy couples was insufficient to insure equilibrium in the high (1100 to 1500°C) temperature. The low temperature phases $\kappa+\theta$ (mp $\sim$ 600°C) would nevertheless have been in equilibrium. If indeed this were another phase, it would prove inconsistent with the phase law since it always appeared with δ. and would subsequently give rise to two, three and four phase regions. The arrangement of these phase regions would also

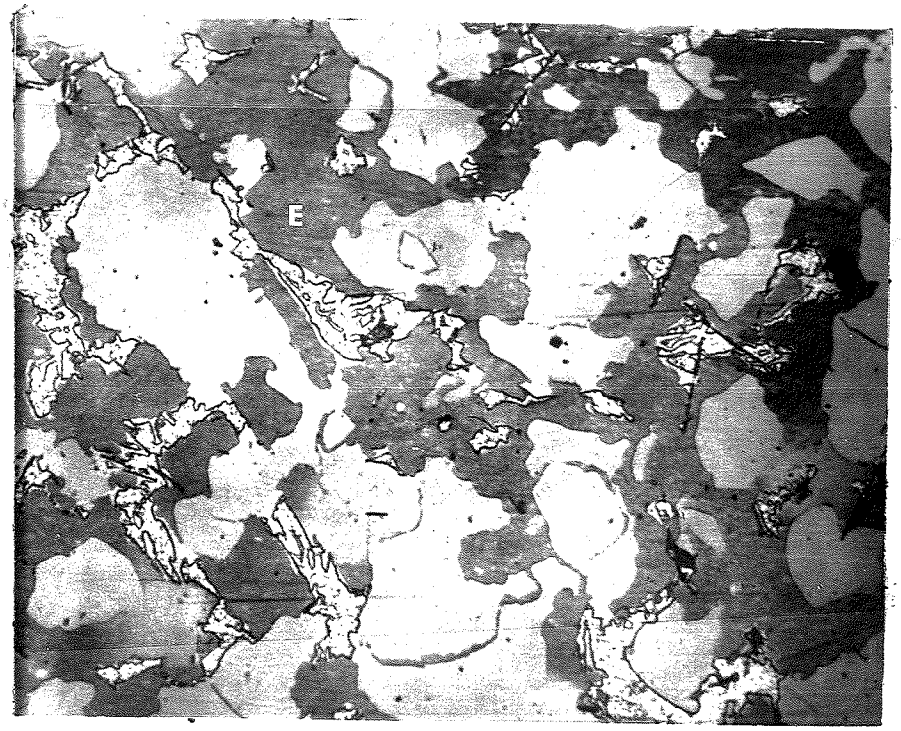

Figure 21b. κ+δ+ε region, heat treated Al-50Ni to Al-33Cu couple, etched 3 secs. in Keller's etch, D = δ, E = ε, K = κ, 500x

Figure 21c. κ+δ region, heat treated Al-50Ni to Al-33Cu couple, etched 3 secs. in Keller's etch, K = κ, X = δ, 500x

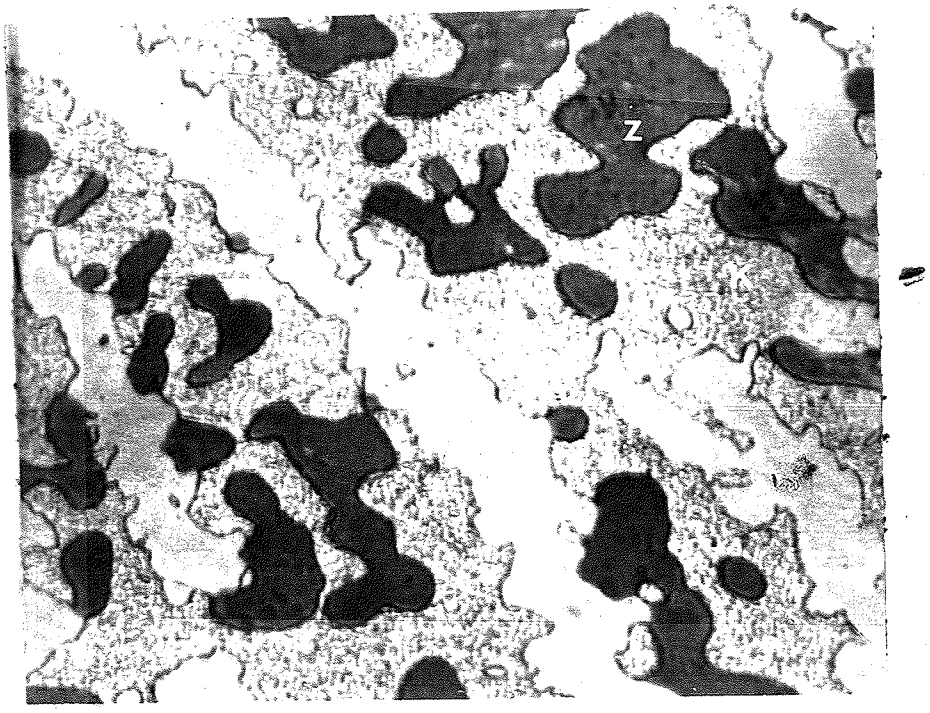

Figure 21d. κ+δ+θ region, heat treated Al-50Ni to Al-33Cu couple, etched 3 secs. in modified Keller's etch, D = δ, K = κ, Z = θ, 500x

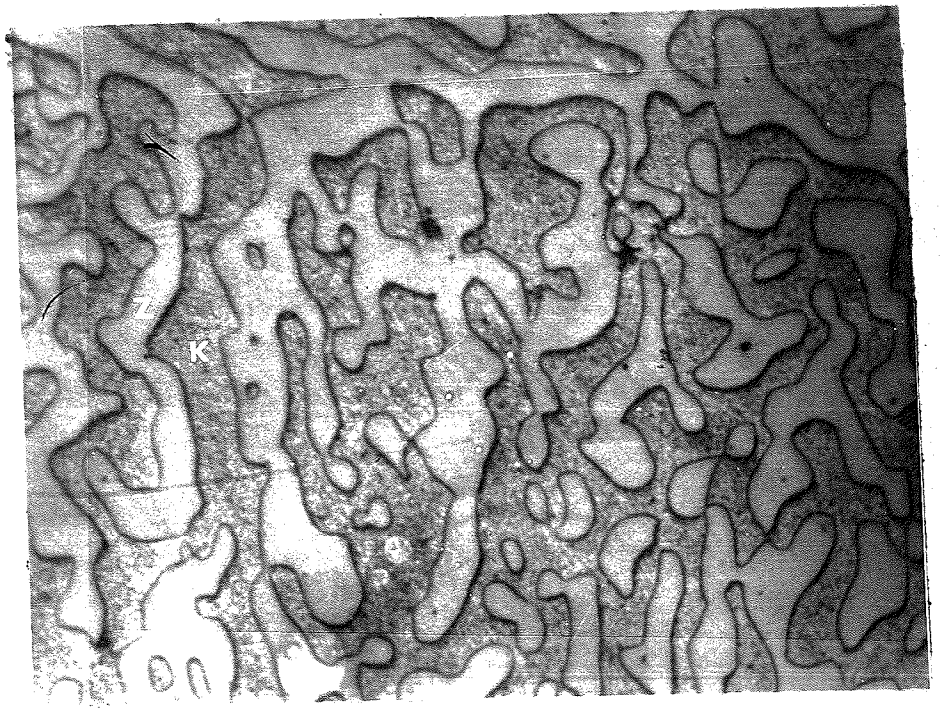

Figure 21e. κ+θ region, heat treated Al-50Ni to Al-33Cu couple, etched 3 secs. in Keller's etch, Z = θ, K = κ, 700x

violate the law of adjoining phases (26). Bradley and Lipson (4) also reported this coring phenomenon in δ.

For probe analysis in the Al-Cu-Ni system no absorption corrections were applied. This was deemed justifiable since the mass absorption coefficients were nearly identical - $\mu_{NiNi} = 59$, $\mu_{NiCu} = 48$, $\mu_{CuCu} = 54$, $\mu_{CuNi} = 64$, $\mu_{AlCu} = 47$, $\mu_{AlNi} = 59$. The difference would result in maximum differences in the intensity function of .5 to 1%.

The concentration gradient in the Al-Cu-Ni couples was not as visually evident as was that in the Al-Mg couples. The gradient was present, however, as the plot of average compositions of the regions sampled fell on or near the straight line joining the end compositions as shown in fig. 22 (Al-18Ni to Al-23Cu).

In a ternary system the concentration gradient may not follow a straight line joining the two initial binary compositions. If the diffusion coefficient of the binary alloying the elements differ appreciably the line will curve. This curvature, however, would be of little consequence since the compositions are measured with the electron microprobe. Moreover, liquid diffusion coefficients are very similar for most elements and it is likely that any curvature would be small. It is not surprising that a straight line joins the Al-Ni and Al-Cu alloys in the present investigation. Cu and Ni are very similar, neighbours in the periodic table, and it is also likely that their diffusion coefficients are very similar.

To establish the extent of each phase field, the compositions of individual phases in three phase regions was used. This is in accordance with the rules of phase diagramming for isothermal sections of ternary diagrams. The results of the probe analysis are contained in Tables VI through IX.

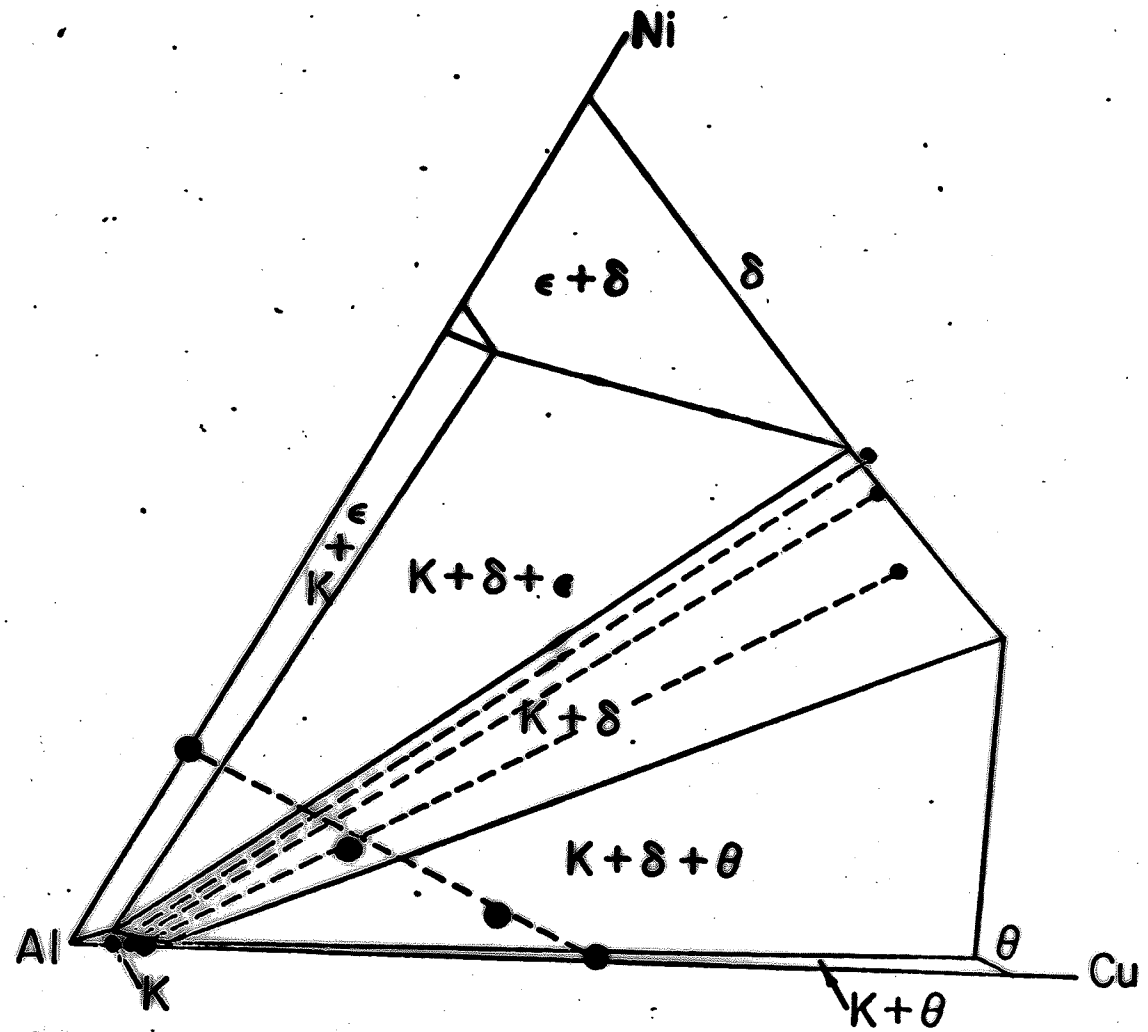

FIGURE 22 AUTHORS ISOTHERMAL SECTION OF Al-Cu-Ni SYSTEM AT 535°C

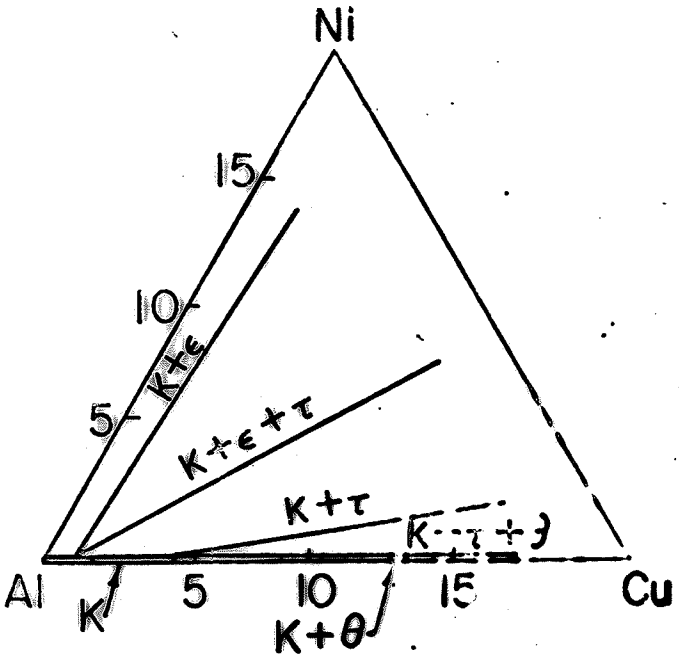

JRE 2 BINGHAM & HAUGHTON'S ( ) ISOTHERMAL
OF Al-Cu-Ni SYSTEM AT 535° C

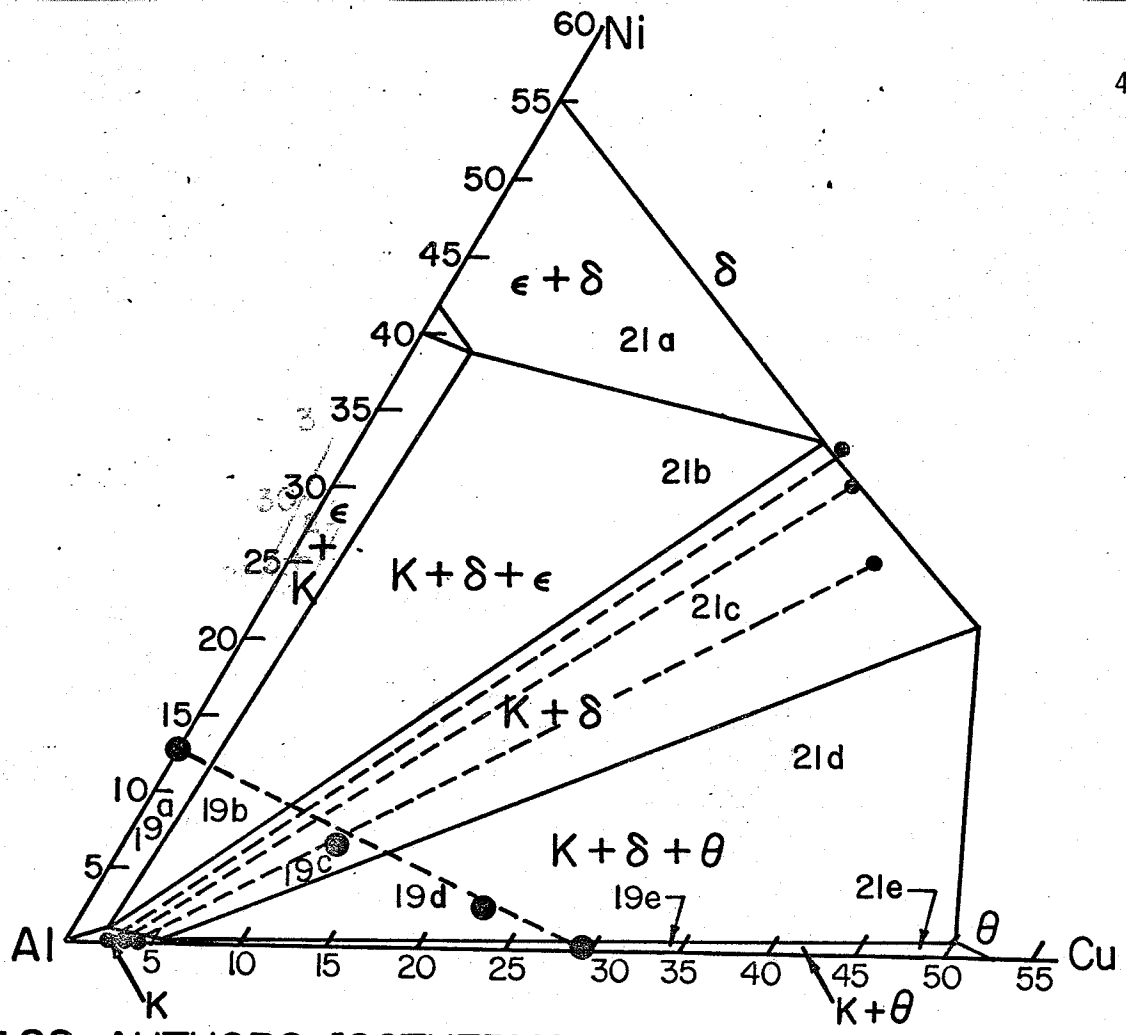

FIGURE 22 AUTHORS ISOTHERMAL SECTION OF Al-Cu-Ni SYSTEM AT 535°C

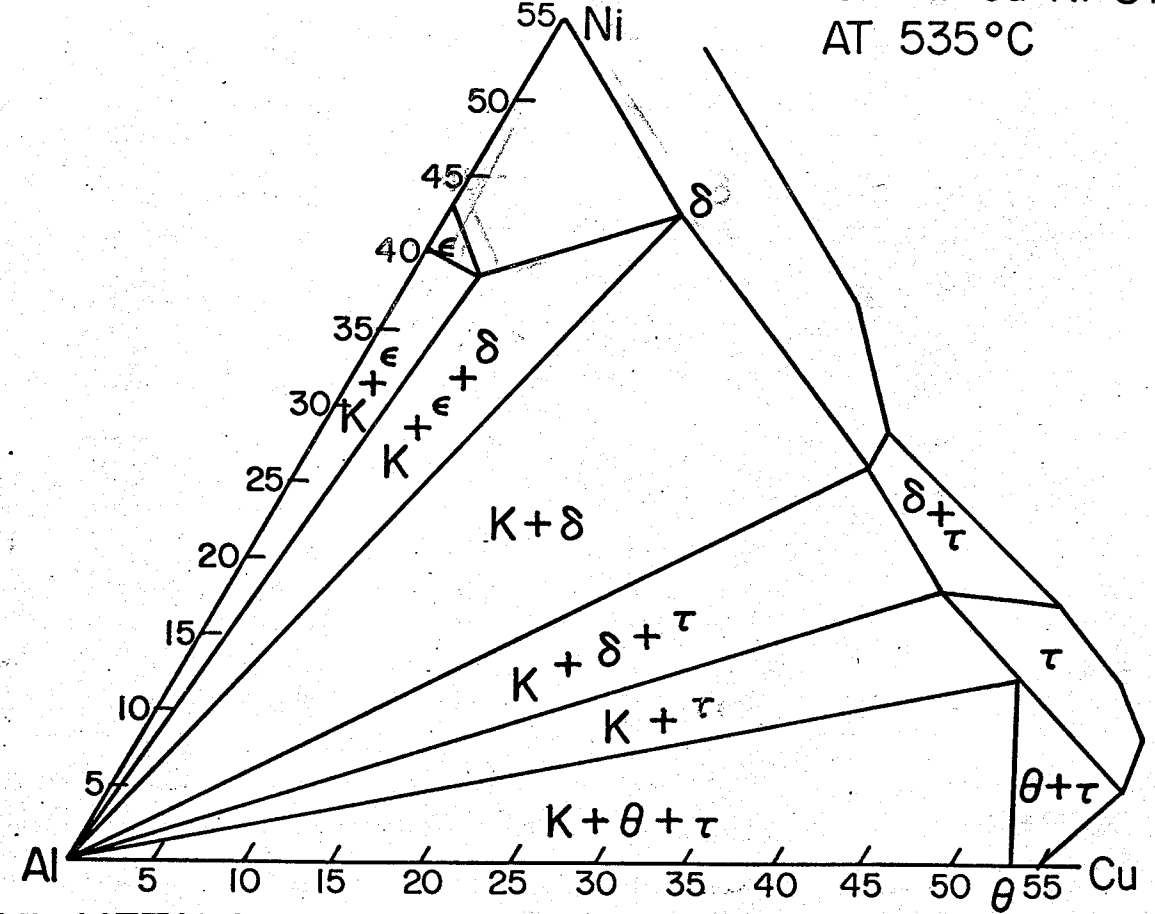

FIGURE 23 METALS HANDBOOK TERNARY (to same scale as authors diagram)

Since several couples were sampled, the average composition of each phase analyzed was used in the construction of the isothermal section at 535°C (fig. 22).

TABLE III Comparison of compositions of phase fields (Author's vs Metals Handbook (18).

Region		κ+δ+ε			κ+δ+θ		
Phase		κ	δ	ε	κ	δ	θ
Average Comp.	Cu	2	26	2.5	5	41	50
Author's	Ni	1	33.5	39	0	21.5	1
Composition	Cu	0	13	4	0	-	53
(18)	Ni	0	43	37	0	-	0

The compositions in the author's diagram are compared where applicable with those of the presently accepted diagram from the Metals Handbook (18) in Table II.

A check on the isothermal section is inherent in the couples that were analyzed. The compositions of the phases in the two phase regions fell within the established boundaries of the two phase regions. For example consider the κ+δ region. The κ and δ compositions in Table VIII from the κ+δ region fall in the κ and δ phases respectively bounded by the tie lines of the two phase region. Furthermore, the tie line between the two individual phases fell in substantially the same directions as the phase boundaries.(see fig. 22, κ+δ region.)

Since several couples were sampled, the average composition of each phase analyzed was used in the construction of the isothermal section at 535°C (fig. 22).

TABLE III Comparison of compositions of phase fields (Author's vs Metals Handbook (18).

Region		κ+δ+ε			κ+δ+θ		
Phase		κ	δ	ε	κ	δ	θ
Average Comp.	Cu	2	26	2.5	5	41	50
Author's	Ni	1	33.5	39	0	21.5	1
Composition	Cu	0	13	4	0	-	53
(18)	Ni	0	43	37	0	-	0

The compositions in the author's diagram are compared where applicable with those of the presently accepted diagram from the Metals Handbook (18) in Table II.

A check on the isothermal section is inherent in the couples that were analyzed. The compositions of the phases in the two phase regions fell within the established boundaries of the two phase regions. For example consider the κ+δ region. The κ and δ compositions in Table VIII from the κ+δ region fall in the κ and δ phases respectively bounded by the tie lines of the two phase region. Furthermore, the tie line between the two individual phases fell in substantially the same directions as the phase boundaries.(see fig. 22, κ+δ region.)

7.3 Liquidus Reactions

Strictly speaking the liquidus surface was not determined, but the liquidus reactions were observed. Since the ternary phase, τ, is not present in the Al (rich) corner of the Al-Cu-Ni system, the reactions are somewhat changed in this regard from fig. 6. The couple that was examined for these reactions was from θ (Al-52%Cu) to Al-18Ni. Proceeding from the Ni (rich) end, ε and the $\kappa + \varepsilon$ eutectic are observed as shown in fig. 24. As the Cu content increases, the ε phase becomes enveloped with δ as shown in fig. 25 and is typical of a $L+\varepsilon \rightarrow \delta$ peritectic reaction. At higher Cu concentrations, δ solidifies first, followed by the $\kappa+\varepsilon$ eutectic and finally a ternary eutectic (fig. 26). It is reasonable to assume that the ternary eutectic comprises κ, θ, and δ but the structure is so fine that the three types of lamellae cannot be distinguished. The Cu rich end of the couple (fig. 27) shows θ, δ and a eutectic, presumably the ternary eutectic. The $\delta+L \rightarrow \varepsilon$ peritectic (fig. 28) was also observed. The $L \rightarrow \varepsilon+\delta$ eutectic separating the two peritectic reactions was not observed but this eutectic reaction occurs over a very limited composition range and would be difficult to observe in the diffusion couples used. It is likely that the liquid-solid reactions are similar to those determined by previous investigators (fig. 6) except that the $L+\delta \rightarrow \tau$ reaction is removed since τ does not exist in the Al (rich) end of the ternary diagram and the $\theta+\tau$ eutectic is changed to the $\theta+\delta$ eutectic.

7.4 Analysis of Previous Research and Accepted Diagram of Al-Cu-Ni System

The original work done on the Al-Cu-Ni system, (2) bears a striking similarity to the author's work. From their vertical sections at

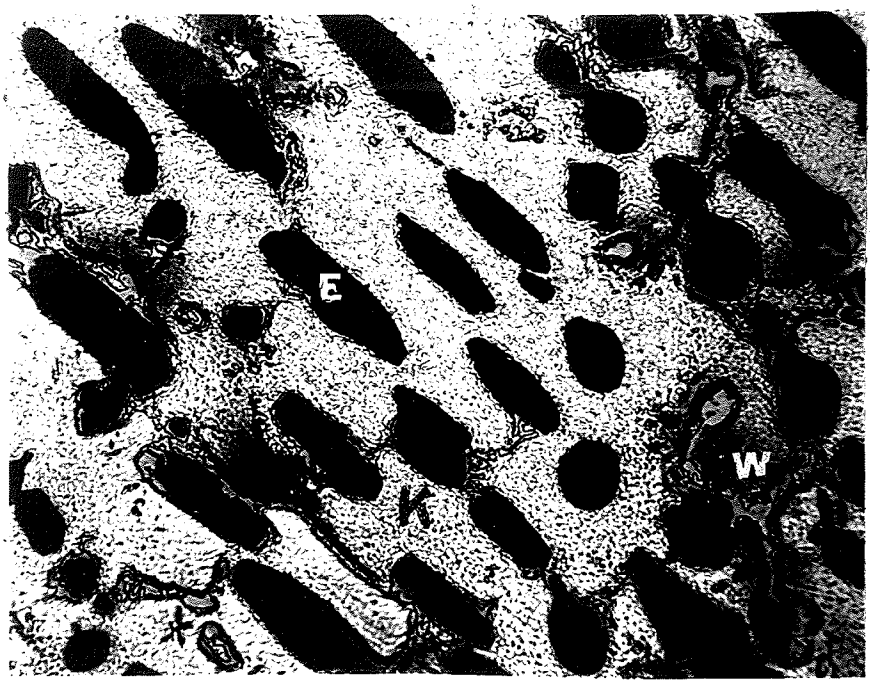

Figure 24. κ, ε, and κ+ε eutectic, as-cast θ to Al-18Ni couple, etched 3 secs. in modified Keller's etch, E = ε, K = κ, W = eutectic, 500x

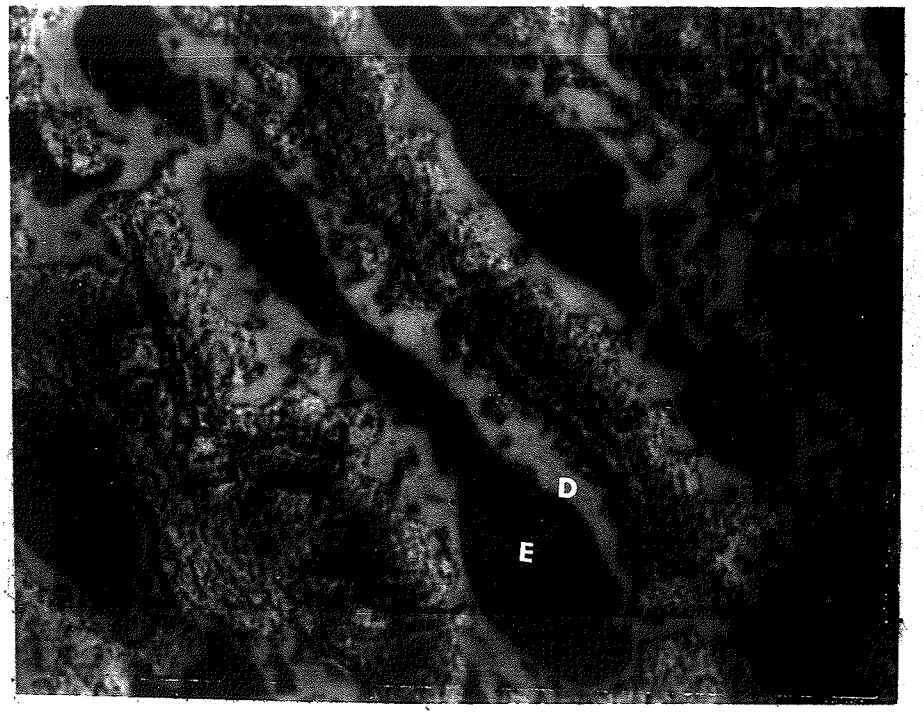

Figure 25. L+ε→δ peritectic, as-cast θ to Al-18Ni couple, etched 3 secs. in modified Keller's etch, E = ε, D = δ, 1300x.

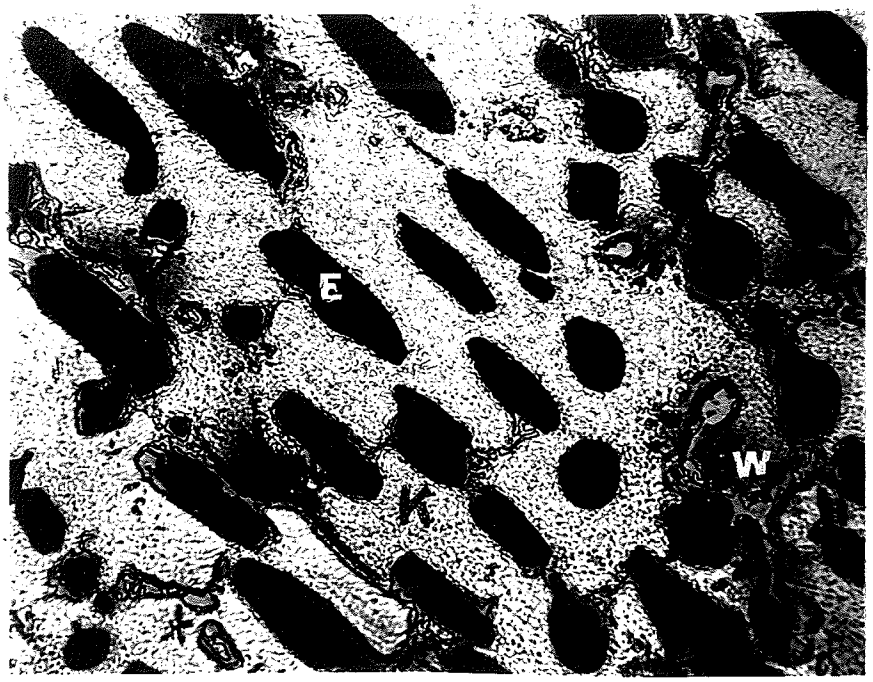

Figure 24. κ, ε, and κ+ε eutectic, as-cast θ to Al-18Ni couple, etched 3 secs. in modified Keller's etch, E = ε, K = κ, W = eutectic, 500x

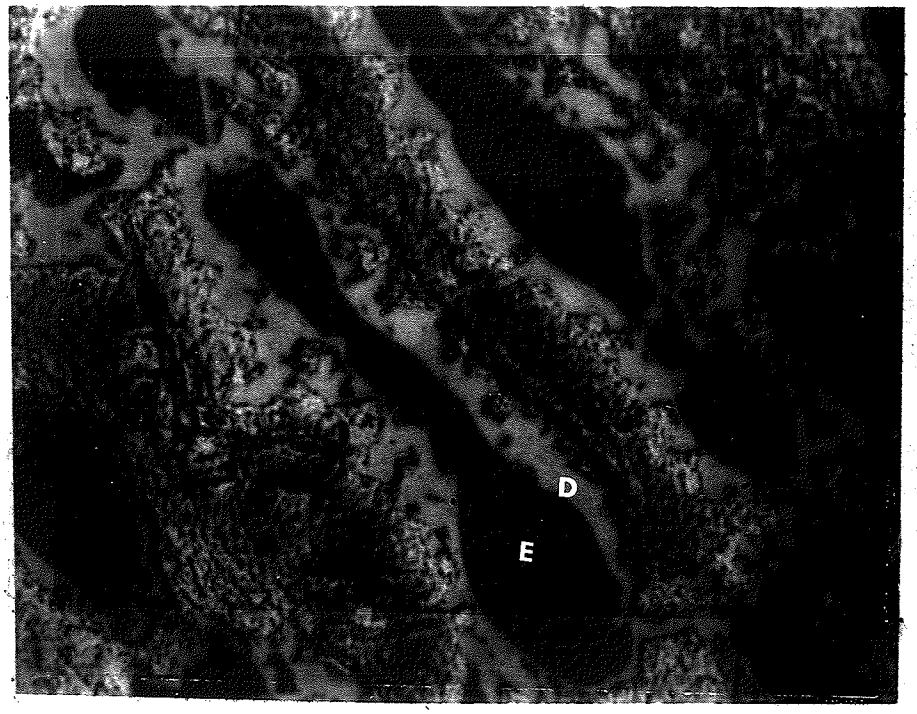

Figure 25. L+ε→δ peritectic, as-cast θ to Al-18Ni couple, etched 3 secs. in modified Keller's etch, E = ε, D = δ, 1300x.

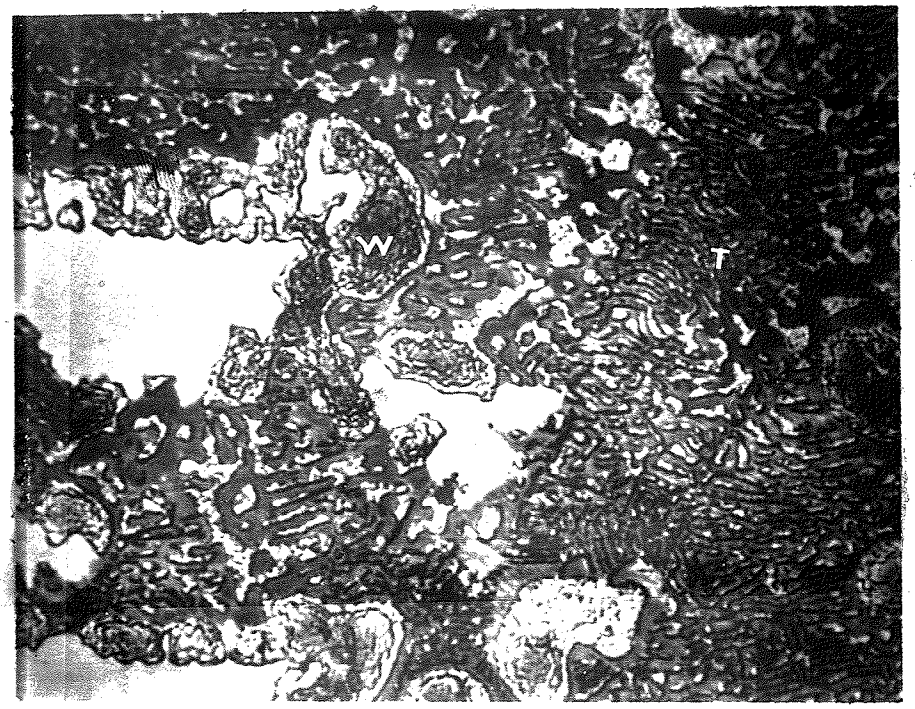

Figure 26. δ, κ+ε eutectic, and ternary eutectic, as-cast θ to Al-18Ni couple, etched 3 secs. in modified Keller's etch, D = δ, W = κ+ε eutectic, T = ternary eutectic, 780x

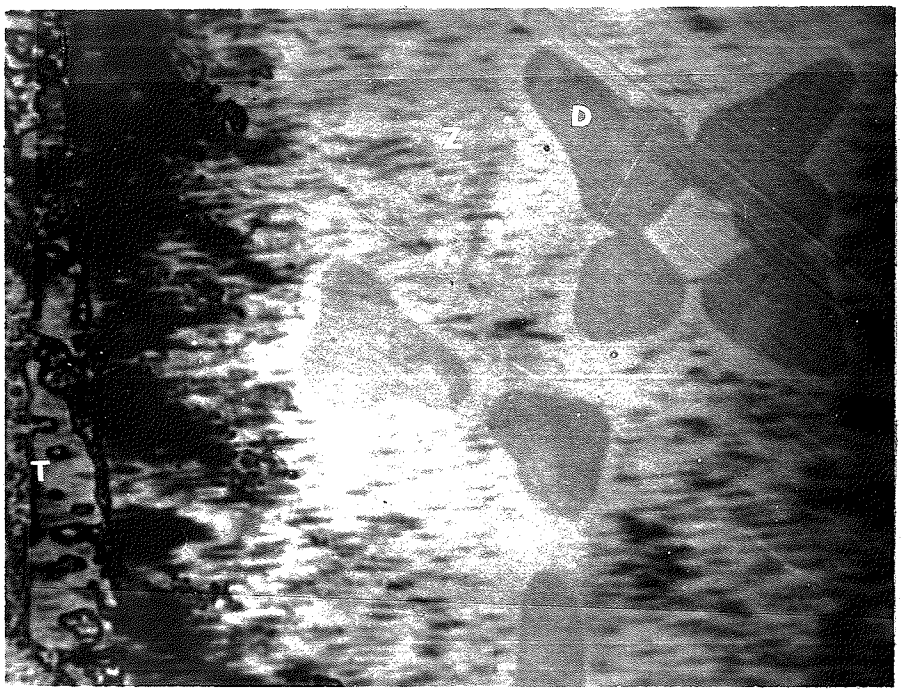

Figure 27. θ, δ and ternary eutectic, as-cast θ to Al-18Ni couple, etched 3 secs. in modified Keller's etch, Z = θ, D = δ, T = ternary eutectic, 1300x

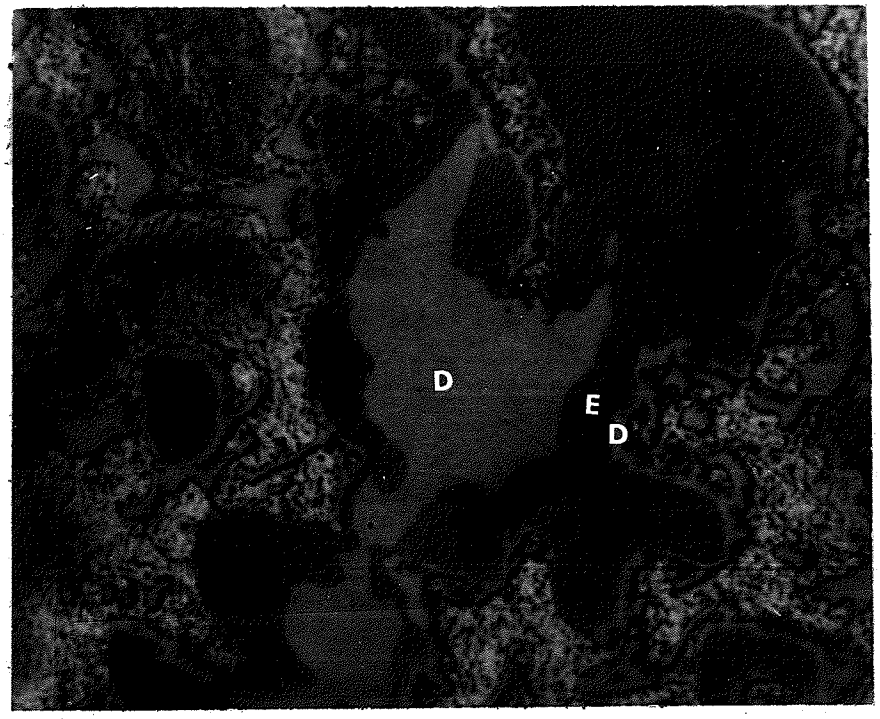

Figure 28. Double peritectic: L+δ→ε and L+ε→δ as-cast to Al-18Ni couple etched 3 secs. in modified Keller's etch, D = δ, E = ε, 1300x

constant copper and constant nickel concentrations the isothermal section of fig. 2 was constructed. If this isothermal section at 535°C were compared to the author's, only minor phase region shift is seen (see comparison fig. 23) and then τ is the author's δ. There are several reasons for believing that τ is in fact δ: (1) The appearance of their τ under various etchants -20%NHO_3, 1% HF is identical to δ.

(2) Bingham and Haughton were working from an incomplete Al-Ni binary diagram and may not have known about δ. Hence they would assume that some unknown phase was a ternary constituent and would be unaware that binary δ could extend into the ternary system.

(3) According to Bradley and Lipson (4), the τ found by Bingham and Haughton at Cu_2NiAl_5 was slightly outside their τ at Cu_3NiAl_6.

Bingham and Haughton had not said that Cu_2NiAl_5 was τ, but that this composition Al-39Cu-18Ni was about 70% τ. This was presumably done from area analysis of a photomicrograph. On the author's isothermal section, this composition is about 80 wt% δ, which due to its greater density, would be less by area on a photomicrograph.

(4) On their vertical sections (2) show a peritectic $L+\varepsilon\rightarrow\tau$, whereas in the Al-Cu-Ni system both (21) and (8) show a $L+\varepsilon\rightarrow\delta$ but never any ε to τ peritectic.

For these reasons, the author believes that Bingham and Haughton had essentially the same diagram as his, only they had mistakingly called δ, τ being unaware that binary δ extended into the ternary diagram.

The accepted phase diagram, as seen in Metals Handbook (18) and Metals Reference Book (22), is not that of Bingham and Haughton (2) but that proposed by Bradley and Lipson (4). From the comparison of their (8) and (4), diagram to the author's great discrepancies can be seen (fig. 23):

(1) The main difference is that the author has no τ phase in the Al end of the Al-Cu-Ni system. This of course leads to great changes to the number and disposition of the phase regions.

(2) The author shows an κ and a $\kappa+\delta$ region in his diagram whereas (18) and (4) do not.

(3) The author's diagram has the δ zone extended further towards the Al-Cu binary than do Bradley and Lipson (4).

(4) There is a difference in extent of the two and three phase regions in the author's diagram and those from (4). This is of course necessary since the author has fewer number of phase regions with the omission of τ.

It should be stated here that the author does not deny the existence of a ternary phase τ, only that the arrangement of tie lines and phase regions is such that τ does not occur in aluminum rich end of the Al-Cu-Ni system.

There are several points about Bradley and Lipson's (4) work which indicate that τ may not really exist in the region they claim:

(1) Their samples were slowly cooled from some annealing temperature - generally around 800^{o}C. The alloys were thus not equilibrium configuration for any particular temperature as are the authors.

(2) They did only X-ray examination. At no time do they refer to photomicrograph, or any other visual technique. They use X-ray for both identification of phases and the location of phase boundaries.

(3) They state that there is extreme similarity between the X-ray patterns of δ, τ and β (a higher nickel phase than δ). In fact there is overlapping of patterns at low order reflections and they admitted difficulty distinguishing between these phases.

(4) They used a camera with 9 cm. diameter. This is a small camera, and not conducive to accurate work.

Furthermore, Bradley and Lipson (4) did not include the κ and $\kappa+\theta$ regions, already established by Bingham and Haughton (2) and required from a theoretical point of view. All these factors indicate that τ may indeed not be present in the Al (rich) end of Al-Cu-Ni system, although the phase itself may be exactly where Bradley and Lipson (4) indicated.

The diagram quoted by Smithells (22) is even more misleading than that of the Metals Handbook (18). He has left out the aforementioned κ and $\kappa+\theta$ regions as well as mislabelling the diagram. Otherwise the diagram is the same as (18).

The work done by Rapp (21) is somewhat more confusing. He has three phases (fig. 5) not present in the author's isothermal section at 535°C - Y, Z and τ, and is missing δ. All the phases Y, Z, and τ are various shades of grey according to Rapp (21) and after some examination of his as cast and heat treated micrographs it would appear apparent that all of the extraneous phases are probably δ. Y is definitely δ as he has shown it at a composition (5 Cu 25 Ni), which is totally in the $\kappa+\delta+\varepsilon$ region, transforming peritectically to ε. The phase he calls Z is likewise seen in peritectic reaction with ε and in the $\kappa+\delta$ region he calls an alloy $\kappa+Z$, hence Z is probably also δ. He refers to a ternary phase τ and shows this phase, supposedly, in the $\kappa+\theta+\delta$ region. Presumably he was influenced by Bradley and Lipson's (4) work and accepted the presence of the ternary phase in the Al (rich) end of the Al-Cu-Ni system.

7.5 Extension and Application of Diffusion Couple Phase Diagramming

The technique involving phase diagramming by microprobe analysis of liquid diffusion couples is no doubt most useful for the quantitative and qualitative analysis of the phase relations in materials systems. By utilizing one set of diffusion couples, the equilibrium phase diagram can be established by different heat treatments up to the solidus of the lowest melting phase. The method is applicable to phase systems of any number of components. Any section can be produced by varying the composition of the ends of the couple, for example holding one or more components constant while varying the other components.

For producing diffusion couples from very reactive, or very high melting point alloys, a zone refiner might be used. Placing the couple in a vertical or horizontal position, to prevent gravitational segregation, a molten zone could be passed along it thus distributing the elements along the length of the diffusion couple. The couple could also be encapsuled in glass or silica to physically stabilize the couple, to isolate it from the atmosphere, or to allow utilization of a wide molten zone.

The liquid diffusion couples would also allow a quick check of a system for structurally feasible alloys. By checking the micro-hardness of phases, their strengths may be anticipated, and their range of composition may be established by the author's method - all in the same diffusion couple.

The method is in general very simple. Temperature control is not required as evidenced by the use of the oxy-acetylene torch for producing couples with different melting point ends. Also by producing a

sufficiently shallow gradient, the phase fields can be made large enough to do X-ray work on them.

8. CONCLUSIONS

The experimental work on the Al-Cu-Ni ternary required about six months. The author's diagram, however, was established in only four weeks working time after the 3/8" diameter diffusion couples were adopted. The author was also influenced by the previous investigations and considerable time was spent trying to confirm the presence of the ternary phase τ in the Al (rich) corner of the Al-Cu-Ni system. Finally, however, it was concluded that τ did not exist there, and the present diagram was established. This absence of τ is the main difference between the author's diagram and presently accepted diagrams, and it significantly alters the appearance of the Al-Cu-Ni phase diagram in the Al(rich) corner.

In the Al-Mg system, the prescence and composition range of ε were confirmed. This phase is stable at least at the heat treated temperature of 380°C between Al-39.5 to 41.5 wt% Mg.

ACKNOWLEDGEMENTS

In completing this work I am very grateful to my advisor Dr. J.R. Cahoon of the Department of Mechanical Engineering, University of Manitoba, for his continuous guidance and good suggestions, to Dr. A. Sawatzky of Atomic Energy of Canada Limited, Pinawa, for the use of electron microprobe facilities, and to the Steel Company of Canada for their generous financial assistance.

BIBLIOGRAPHY

(1) Austin, C.R., Murphy, A.J.; "The Ternary System Copper-Aluminum-Nickel", Journal of The Institute of Metals (London) V. 29, 1923, p. 327.

(2) Bingham, K., Haughton, J.L.; "The Constitution of Some Alloys of Aluminum with Copper and Nickel"; Journal of the Institute of Metals (London) V. 29, 1923, p. 71.

(3) Birks, L.S.; Electron Probe Microanalysis Interscience Publishers, 1963, New York.

(4) Bradley, A.J.; Lipson, H.; "An X-ray Investigation of Slowly Cooled Copper Nickel-Aluminum Alloys" Proceedings of The Royal Society (London) 167, p. 421 (1938).

(5) Brown, J.B.; "NewApplications of Electron Probe Microanalysis", Fifty Years of Progress in Metallographic Techniques, ASTM STP 430, Am. Soc. Test. Materials, 1968, pp. 359-382.

(6) Criss, J.W.; "Progress in Quantitative Electron Probe Micro-analysis", Fifty Years of Progress in Metallographic Techniques, ASTM STP 430, Am. Soc. Test. Materials, 1968, pp. 291-314.

(7) Doan, A.S.; Goldstein, J.I.; "The Ternary Phase Diagram Fe-Ni-P", Metallurgical Transactions,Vol.1, June 1970, p. 1759.

(8) "Equilibrium Diagrams of Aluminum Systems", The Aluminium Development Association, London, 1961, p. 67.

(9) Gordon, P.; Principles of Phase Diagrams in Materials Systems, McGraw-Hill, New York, 1968.

(10) Hansen, M.; Constitution of Binary Alloys, McGraw-Hill, New York, 1958, 2nd Ed.

(11) Hansen, M.; Kessler, H.D.; McPherson, D.J.; "The Titanium Silicon System", Transactions of the American Societies for Metals (44), 1952, p. 518.

(12) Hume-Rothery, W.; Christian, J.W.; Pearson, W.B.; Metallurgical Equilibrium Diagrams, The Institute of Physics, London, 1952.

(13) Kaufman, L.; Bernstein, H.; Computer Calculations of Phase Diagrams, Academic Press, N.Y., 1970.

(14) Kidson, G.V.; Miller, G.D.; "A Study of the Interdiffusion of Aluminium and Zirconium", Journal of Nuclear Materials 1,12 (1964) pp. 61-69.

(15) Lemkey, F.D.; Hertzberg, R.W.; and Ford, J.A.; "Microstructure Crystallography and Mechanical Properties of Unidirectionally Solidified Al-Al_3Ni Eutectic" TMS-AIME, 233, 1965, p. 334.

(16) Levin, E.M.; Robius, C.R.; and McMurdie, H.F.; Phase Diagrams for Ceramists, American Ceramic Society, Columbus, Ohio 1964.

(17) MacChesney, J.B.; Rosenberg, P.E.; "The Methods of Phase Equilibrium Determination and Their Associated Problems", Phase Diagrams: Materials Science and Technology, vol.1, Academic Press, New York, 1970.

(18) Metals Handbook, American Society for Metals, 1948.

(19) Purdy, G.A.; McMaster University, Hamilton, Personal Communication.

(20) Rao, Y.K.; "Thermodynamics of Phase Diagrams", Phase Diagrams: Materials Science and Technology, vol. 1, Academic Press, New York, 1970.

(21) Rapp, A.; "Aluminium Corner of The Ternary System Aluminium-Copper-Nickel", Aluminium Archiv, Band 28, 1940.

(22) Smithells, C.J.; Metals Reference Book, vol. 1, 3rd Ed. Butterworths, Washington.

(23) Thomas, G.; Transmission Electron Microscopy of Metals, John Wiley and Sons, New York, 1963.

(24) West, D.R.F.; Ternary Equilibrium Diagrams, MacMillan Co. London, 1965.

(25) Yakowitz, H.; "Evaluation of Specimen Preparation and the Use of Standards in Electron Probe Microanalysis", Fifty Years of Progress in Metallographic Techniques, ASTM STP 430, Am. Soc. Test. Materials, 1968, pp. 383-408.

(26) Yeh, H.C.; "Interpretation of Phase Diagrams", Phase Diagrams: Materials Science and Technology, Academic Press, New York, 1970.

APPENDIX A.

Probe Data and Analysis

A1. Al-Mg System

TABLE NO. IV

Al-Mg Couple, Heat Treated

Phase Boundary	Counts (2 seconds)	Distance (in.)	Comment
δ to $\delta+\gamma$	3,300	.490	1. All readings corrected for background.
$\delta+\gamma$ wt	19,700	-	
$\delta+\gamma$ to γ	22,100	.312	2. $K_{\alpha 1}$ Aluminium peak, 20 Kw electrons.
γ to $\varepsilon+\gamma$	30,100	.247	
$\gamma+\varepsilon$ to ε	-	.241	3. Area at phase boundary analyzed.
ε to β	50,000	.236	
β to $\alpha+\beta$	51,000	.169	
$\alpha+\beta$ to α	101,400	.05	

TABLE NO. V

Al-Mg, Heat treated, average composition = 42% Mg

Phase Region	Phase	Counts (2 seconds)	Composition	Comment
β	β	9040	63 wt% (std.)	1. Composition Calc. using Absorption correction as per Birks (3).
γ	γ	6600	52.5 wt%	
$\beta+\gamma$	"ε" near γ	8270	60.5 wt%	2. counts corrected for background.
β γ	"ε" near β	8080	58.5 wt%	3. $K_{\alpha 1}$ Al peak, 20 Kw electrons.
				4. β used as std. @ 63 wt% Al.

A.1 Calculation of Composition

The calculation method is taken from Birks (3). It is used to correct for the absorption of Al radiation in Mg and vice versa.

$$I_{Al}/I_{100Al} = w_{Al}F_{Al}/F_{100Al} \quad (1)$$

where I_{Al} = intensity of radiation at any composition as measured in counts.

I_{100Al} = intensity of radiation from pure aluminum.

w_{Al} = composition of Al in alloy producing I_{Al}.

F_{Al} = intensity function for Al in alloy.

F_{100Al} = intensity for pure Al.

hence: from eq. 1

$$I_{Al}/I_{\beta Al} = w_{Al}F_{Al}/w_{\beta Al}F_{\beta Al} \quad (2)$$

where $w_{\beta Al} = .63$

$I_{\beta Al} = 9040$

and to find $F_{\beta Al}$: using tables for intensity function from Birks (3):

$$\mu_\beta' = .37\ \mu_{MgAl} + .63\ \mu_{AlAl}$$

μ_β' = total mass absorption coefficient for characteristic radiation from aluminum in β.

μ_{MgAl} = mass absorption coefficient of Mg for characteristic radiation from Al.

= 4300

μ_{AlAl} = mass absorption coefficient of Al for characteristic radiation from Al.

$= 300$

$\mu'_{\beta} = .37(4300) + .63(300) = 1590 + 190$

$= 1780$

$\mu'_{\beta} \csc \psi = 1780 \times \csc 38.5\%$

$= 2860$

ψ = take off angle for measuring X-rays.

$F_{\beta Al} = 50.3$

Now for example to find $w_{\gamma Al}$: from eqs. (1) and (2)

$$\frac{I_{\gamma Al}}{I_{\beta Al}} \quad \frac{w_{\beta Al} F_{\beta Al}}{F_{\gamma Al}} = w_{\gamma Al} \qquad (3)$$

$F_{\gamma Al}$: Assume $w_{\gamma Al} = .53$

$\mu'_{\gamma Al} = .47(4300) + .53(300)$

$= 2170$

$\mu_{\gamma Al} \csc \psi = 2170 \times 1.61$

$= 3500$

$F_{\gamma Al} = 44.3$

$w_{\gamma Al} = \frac{6600}{9040} \cdot \frac{50.3}{44.3} \cdot 0.63 = 52.5$ wt% Al.

TABLE NO. VI

Al-Mg, heat treated 1 wk.at 380°C.

Region	Phase	Counts (2 sec)	Composition (wt%)	Comments
$\alpha+\beta$	β	20026	64	1. composition calculated as per Birks (3)
	α	40690	90.5	
$\varepsilon+\gamma$	ε	17468	60	2. counts corrected for background
	γ	14380	54	3. $K_{\alpha 1}$ Al peak, 20 Kw electron
$\gamma+\delta$	γ	9678	42	4. Pure Al used as standard
	δ	2208	12.5	
Pure	Al	53000	-	

Calculation of composition as in Al.1

A-2 Al-Cu-Ni System

TABLE NO. VI IA1-23Cu to Al-18Ni -Heattreated for 3 wks at535°C.

Region	Phase	Counts/10 second		Composition (wt%)		Comments
		Cu	Ni	Cu	Ni	
	ε	-	69,674	-	42	Standardize Ni
ε+κ						
	avg.	-	22,145	-	13.4	
κ+δ	δ	34,602	51,889	28	31.2	just inside 2ϕ
	θ	63,906	1,563	51.5	0.95	at boundary with δ+α
κ+δ+θ						
	δ	50,472	34,051	40.8	20.6	middle of 2
δ+κ						phase region
	κ	5,334	20	4.3	-	middle of 2
	κ	7,772	0	6.25	0	
κ+θ	θ	64,319	775	52	0.4	standard for Cu
	avg	37,632	301	30.5	0.2	

The comments are standard for Al-Cu-Ni analysis.

(1) Correction for background made

(2) $K_{\alpha 1}$ peaks of Cu and Ni used for analysis.

(3) No absorption correction employed.

TABLE NO. VIII

Al-23Cu to Al-18Ni - Heat treated for 3 wks at535°C

Region	Phase	Counts/10 seconds		Composition (wt%)		Comments
		Cu	Ni	Cu	Ni	
	θ	47,326	-	52	-	high Cu end, standardize Cu @ 52%
κ+θ	κ	5,068	-	5.5	-	
	avg.	26,250	-	29	-	
	κ	4,786	-	5.3		
	δ	34,367	40,400	37.8	23.2	
κ+δ+θ						
	θ	44,980	1,539	49.4	0.9	
	avg	20,618	3,948	22.7	2.3	
	κ	2,266	0	2.5	0	
κ+δ	δ	23,900	60,669	26.2	34.7	near κ+δ+ε
	avg	-	10,147	-	5.8	
	ε	0	73,200	-	42	standardize Ni @ 42%
κ+ε	κ	-	200	-	0.1	
	avg	-	21,562	-	12.4	
	ε	1,248	63,536	1.4	36.5	
	δ	23,662	56,700	26	32.5	
κ+δ+ε						
	κ	1,194	0	1.3	0	
	avg					
	κ	3,670	0	4.0	0	
κ+δ	δ	29,600	44,475	32.5	25.5	middle of κ+δ region
	avg	11,134	10,930	12.2	6.3	

TABLE IX

Al-50 Ni to Al-33 Cu, Heat treated for 1 wk at 535^0C, at high Ni end.

Region	Phase	Counts/10 seconds		Composition (wt%)		Comments
		Cu	Ni	Cu	Ni	
	δ	7,010	41,790	5.3	52.2	
δ+ε	ε	2,775	33,650	2.3	42	Std. = Ni @ 42%
	avg	5,320	30,280			No good-since Ni avg. below both ε and δ.
	κ	3,050	1,960	2.5	2.5	Ni is high.
	δ	14,935	40,020		50	δ not at equilibrium
κ+δ+ε						
	ε	2,935	32,850	2.5	41	
	avg	17,715	25,505	22.1	19.7	
	κ	5,340	30	4.1	0	
κ+δ	δ	29,890	32,320			not good, δ not at equilibrium
	avg	21,080	7,605	18	9.5	
	κ	8,840	0	6.8		
	δ	39,860	26,220	30.8	32.7	notat equilibrium
κ+δ+θ						
	θ	64,140	755	49.5	1.0	Standard Cu.
	avg	33,830	2,870	26	4	

Note: The copper standard was derived from θ in the three phase region. The θ was assumed to be of uniform composition in the κ+δ+θ region, and the composition of θ could thus be carried over from the high Cu end of the couple to the high Ni end.

The nickel standard was transferred similarly using the composition of δ in the 3-phase region. This value checks very well with the figure that would be obtained if the average nickel content in the κ+δ+θ phase was used as a basis for the standard transfer.

TABLE X

Al-50Ni to Al-33Cu, Heat treated for 1 wk at535^{0}C.

High Cu end.

Region	Phase	Counts/10 seconds		Composition (wt%)		Comments
		Cu	Ni	Cu	Ni	
	κ	6,300	40	5.25	0	
	δ	54,120	11,860	45.5	19.5	
κ+δ+θ						
	θ	57,785	630	48.4	1	
	avg	31,160	3,250	26	5.3	
	κ	6,140	0	5.1	0	
	δ	48,690	13,360	40.8	22	Std. Ni
κ+δ+θ						
	θ	59,110	690	49.5	1	
	avg	33,860	3,250	28.4	5.3	
	κ	7,240	0	6.0	0	
κ+θ	θ	60,640	680	51	1	
	avg	35,370	280	29.5	0.4	near κ+θ+δ region
	κ	7,285	0	6.1		
θ	θ	62,050	200	52	0.33	Standard Cu
	avg	36,070	80	30	0	near end of couple